Tetrahedron 67 (2011) 9639–9667

Contents lists available at SciVerse ScienceDirect

Tetrahedron

journal homepage: www.elsevier.com/locate/tet

Tetrahedron report number 957

Recent advances in acyclic stereocontrol

Alexander G. O'Brien *,†

Department of Chemistry, Imperial College London, South Kensington Campus, London SW7 2AZ, UK

ARTICLE INFO

Article history:
Received 19 September 2011
Available online 6 October 2011

Contents

1. Introduction

1.1. Background and scope of review

The issue of stereochemical control is central to the development of organic synthesis; in particular, the influence of a pre-existing stereocentre upon the new stereocentres established during a reaction is of key importance. Control of the relationship between two or more stereocentres is readily achieved in cyclic systems in which rigorous conformational constraints are imposed, while control of the relationship between stereocentres is more difficult to achieve in acyclic systems that lack such conformational rigidity. Nevertheless, in the 117 years since Fischer's original report on the stereoselective addition of hydrogen cyanide to aldoses,[1] the patterns governing acyclic stereocontrol have been intensely investigated and modelled. As a consequence of the continuing development of new stereoselective reactions and advances in computational techniques, this remains an active area of interest in organic synthesis, with direct relevance to both the synthesis of small molecules and complex biologically active targets.

* Tel.: +49 (0) 30 838 59562; e-mail address: alexander.obrien@mpikg.mpg.de.
† Present address: Department of Biomolecular Systems, Max Planck Institute of Colloids and Interfaces, Arnimallee 22, 14195 Berlin, Germany.

0040-4020/$ – see front matter
doi:10.1016/j.tet.2011.10.002

This review concentrates on the development of models for predicting the sense of acyclic stereocontrol, particularly over the last 10 years. Three major classes of reaction have been reviewed: addition of nucleophiles to carbonyls, addition of both electrophiles and nucleophiles to C=C double bonds, and pericyclic reactions. A brief account of acyclic stereocontrol in reactions of functional groups adjacent to organometallic complexes is given. We concentrate only on the relationships between adjacent stereocentres. Remote acyclic stereocontrol is beyond the scope of this review. Reactions involving chiral auxiliaries, and strategies for establishing absolute asymmetric induction are not covered.

1.2. Stereochemical definitions

The term 'acyclic stereocontrol' appears to have a somewhat flexible definition in the literature, and below is an attempt to define the term. While a particular reaction may establish a relationship between stereocentres in an acyclic molecule, this can be a result of highly ordered cyclic transition states. As an example, the relationships between pseudoequatorial and pseudoaxial substituents in cyclic Zimmerman–Traxler transition states that determine stereoselectivity in the aldol reaction are an example of cyclic stereocontrol,[2] while the stereoselectivity of nucleophilic addition to a carbonyl adjacent to a stereocentre is an example of acyclic stereocontrol (Scheme 1).

Therefore, acyclic stereocontrol refers to reactions where the reacting moiety is free to undergo rotation relative to a pre-existing stereocentre, but adopts a preferred reactive conformation. Reaction can then occur from either one of two diastereotopic faces, as determined by transition state interactions.

2. Nucleophilic addition to carbonyls with adjacent stereocentres

2.1. Historical basis of models

Although the historical development of this area has been comprehensively reviewed,[4] a brief overview is given here in order to aid further discussion, particularly as recent discussions of stereocontrol remain based on these models. In 1952, Cram reported an analysis of 1,2-asymmetric induction in the addition of nucleophiles to carbonyl compounds bearing an adjacent stereocentre **5** to give alcohols **6**.[5] In this case, the largest (L) group adopts a conformation *anti* to the carbonyl group for steric reasons. The nucleophile then attacks preferentially from the side of the small (S) substituent. The outcome of the reaction is modified if chelation (usually mediated by a metal) between the carbonyl oxygen and one of the substituents on the adjacent stereocentre is possible. The large (L) substituent now eclipses the carbonyl group, yet attack still preferentially occurs from the side of the small (S) substituent (Scheme 3).

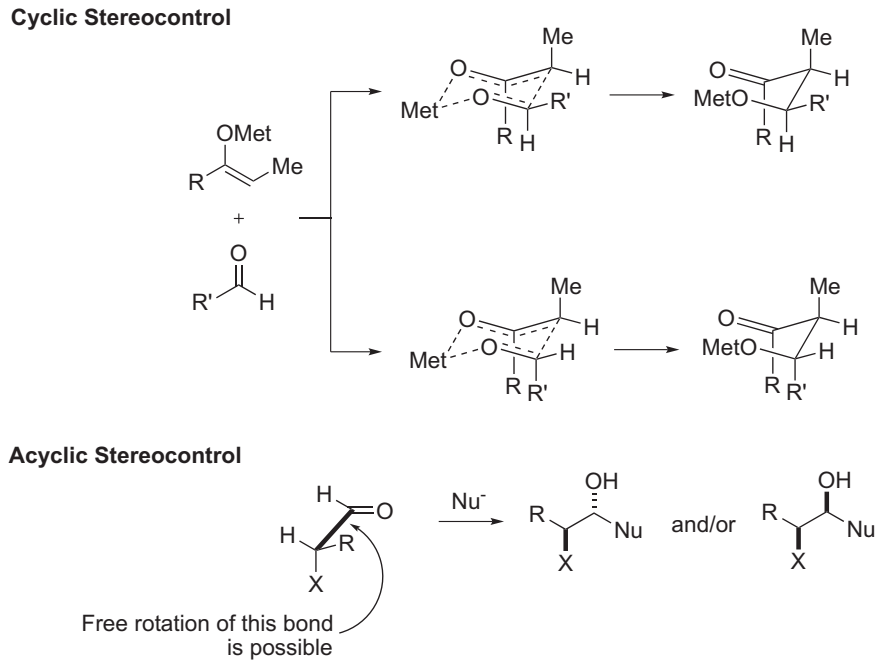

Scheme 1.

A similar dichotomy is shown in the two Claisen rearrangements of **1** in Scheme 2. Although both result in acyclic products **2**, in the former example (Ireland–Claisen rearrangement) the relative configuration of the two new stereocentres formed during the sigmatropic process is controlled by the relative geometries of the vinylic and allylic portions of the ketene acetal, as the reaction occurs via a cyclic transition state.[3] Conversely, as will be discussed in depth in this review, the relationship between a stereocentre outside the pericyclic array and the new C–C bond formed during a Claisen rearrangement **3**→**4** is a function of acyclic stereocontrol.

The Cram model is generally reliable in its explanation of the diastereoselectivity of carbonyl addition reactions, unless polar substituents are present on the adjacent stereocentre. Cornforth, studying the reaction of Grignard reagents and alkyllithiums with α-chloroketones **7** to give alcohols **8**, noted that the α-chloro group took the role of the large substituent, even if more sterically demanding substituents were also present.[6] In a Cram-type model, this represents a nearly eclipsing arrangement between the carbonyl dipole and the C–Cl bond. The conformation with an antiparallel alignment of the C=O and C–Cl dipoles was suggested. In

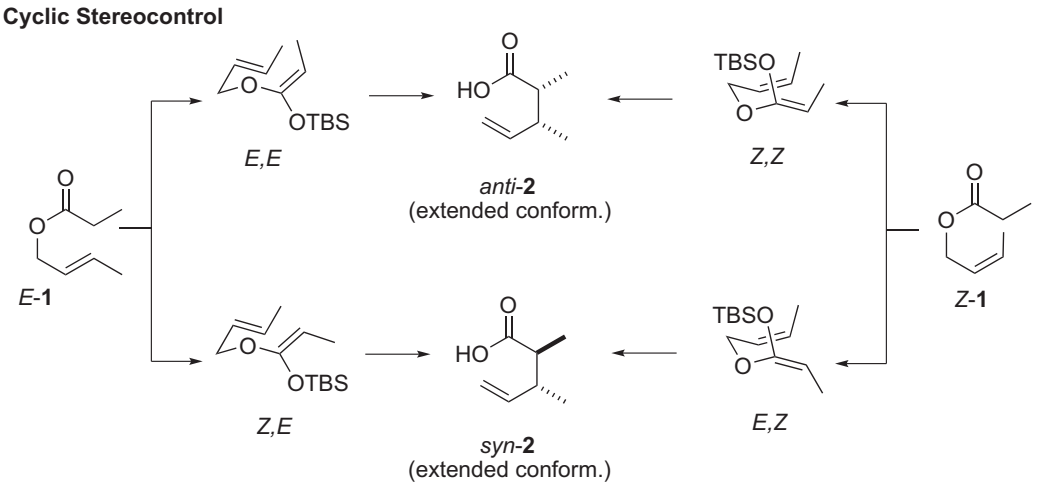

Scheme 2.

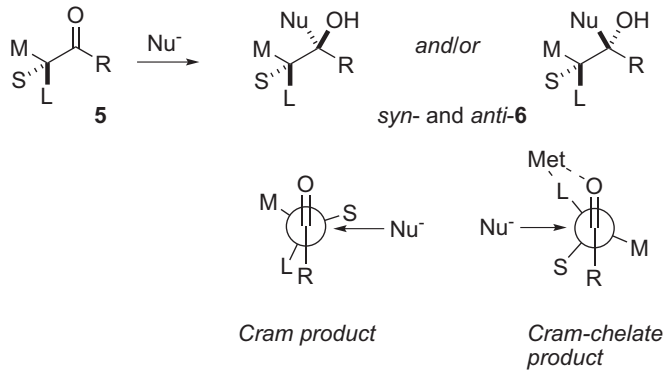

Scheme 3.

the same fashion as the Cram model, attack of the nucleophile then occurs from the side of the smaller substituent (Scheme 4).

Karabatsos suggested a transition-state model **10** and highlighted the importance of the nucleophile attacking along the less hindered trajectory.[7] An alternative interpretation was given by Felkin,[8] who suggested that, if either a Karabatsos or Cram-type transition state was assumed, increasing the size of the large group would lead to a reduction in stereoselectivity, due to strain-between the L and R substituents. This is not borne out experimentally and an investigation into lithium aluminium hydride reduction of ketones adjacent to a stereocentre, in combination with an examination of polar effects, suggested the reaction was best described by a staggered transition state **11**. In this case, the largest, or most electronegative, group lies perpendicular to the plane of the carbonyl, antiparallel to the approach of the nucleophile. Additionally, the staggered Felkin transition state **11** is preferable to the analogous Cram transition state **9** in that it leads directly to the more stable staggered conformation of the product (Scheme 5).

Refinements to the model were made by Anh and Eisenstein,[9] who investigated the individual factors involved in attack of the nucleophile antiperiplanar to the largest or most donating group. Arrangement of the C2–L bond perpendicular to the carbonyl group results in overlap of the C2–L σ^* and C=O π^*orbitals, lowering the energy of the LUMO. Antiperiplanar attack of the nucleophile then gives a more favourable overlap with the combination of orbitals than *syn*-periplanar attack (Scheme 6).

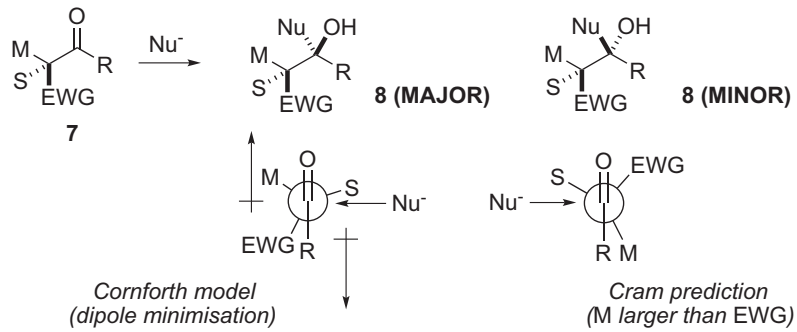

Scheme 4.

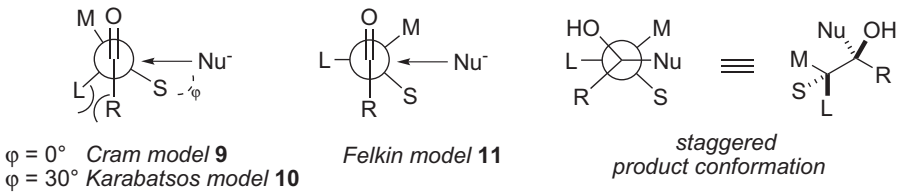

Scheme 5.

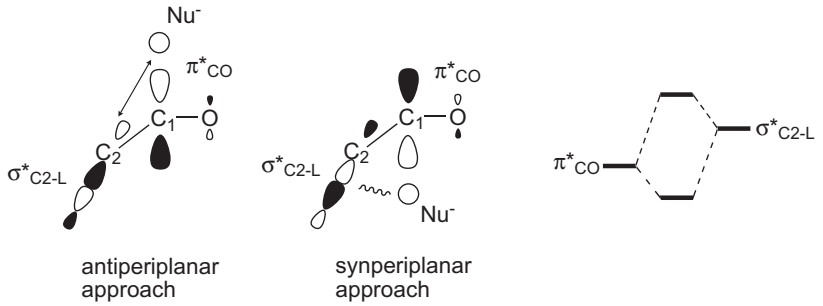

Scheme 6.

Computational evidence suggested that the Bürgi–Dunitz angle[10] should be taken into account (Scheme 7), in agreement with approach of the nucleophile along the least hindered trajectory, reconciling the model with those of Cram and Karabatsos. The combination of the above refinements is now referred to as the polar Felkin–Anh model, and it persists as a widely accepted explanation for acyclic stereocontrol in the addition of nucleophiles to carbonyls with adjacent stereocenters.

reactions of boron enolates derived from ketones with aldehydes bearing an adjacent stereocentre. Mengel and Reiser have reviewed earlier work in this area.[4d] In these reactions, the stereoselectivity has been rationalised using a combination of the Zimmerman–Traxler and Felkin–Anh models. This is an example of acyclic stereocontrol occurring adjacent to a well-defined, cyclic transition state. Parallels can be drawn with exopericyclic stereocontrol in sigmatropic rearrangements, for which similar transition states are proposed.

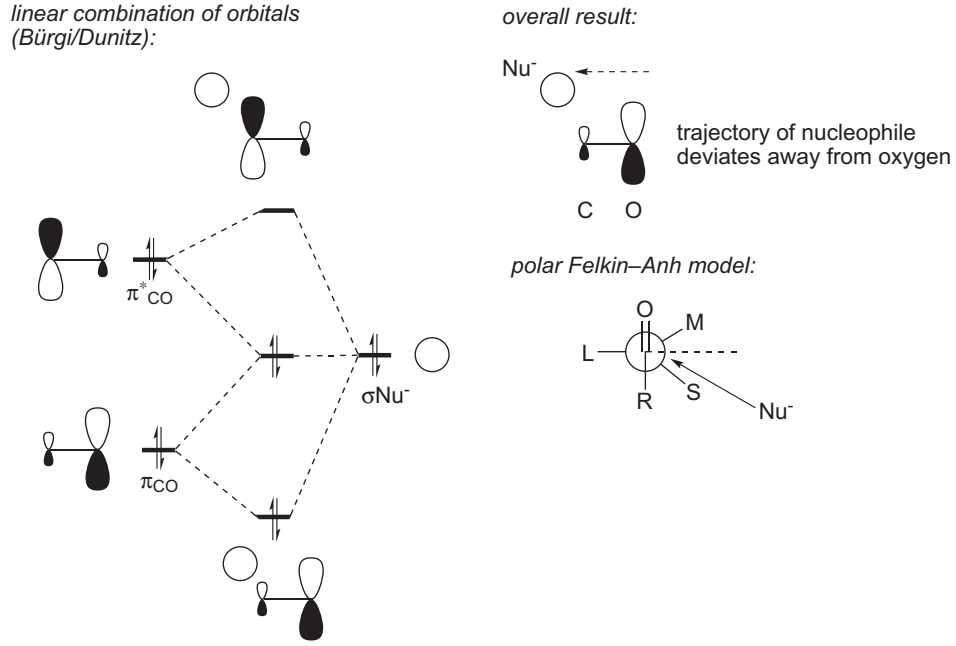

Scheme 7.

2.2. Acyclic stereocontrol adjacent to cyclic transition states

The most important recent developments in attack on carbonyls with an adjacent stereocentre have arisen from investigations into allylborations of aldehydes with an adjacent stereocentre, and aldol

Both Roush[11] and Gennari[12] have discussed this area. A transition state analysis is presented in Scheme 8. For each reaction of aldehyde **12** with *E*- or *Z*-enolates, Zimmerman–Traxler transition states establish the relationship between C2 and C3 in product **13** in line with the prediction. The relationship between C3 and C4 is

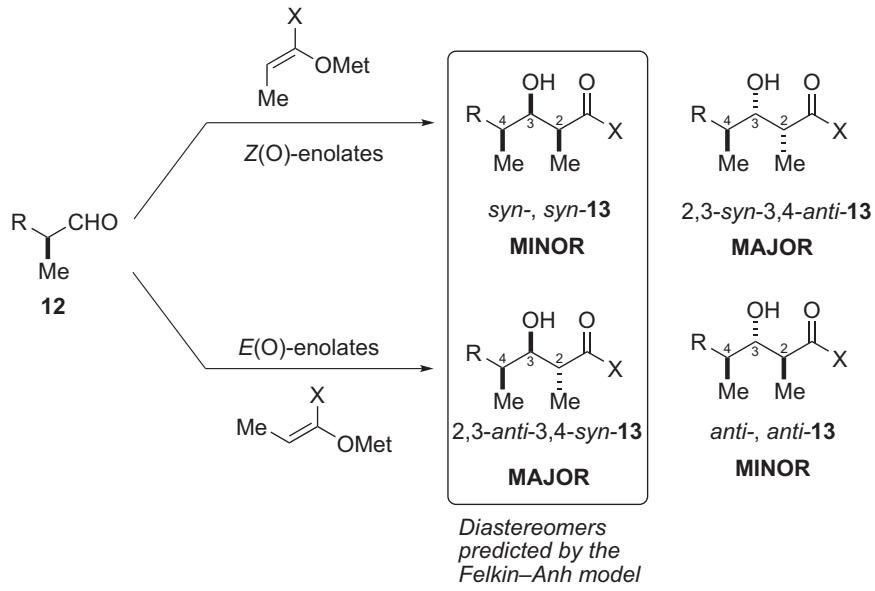

Transition States for *Z*(O)-Enolate Aldol Reactions

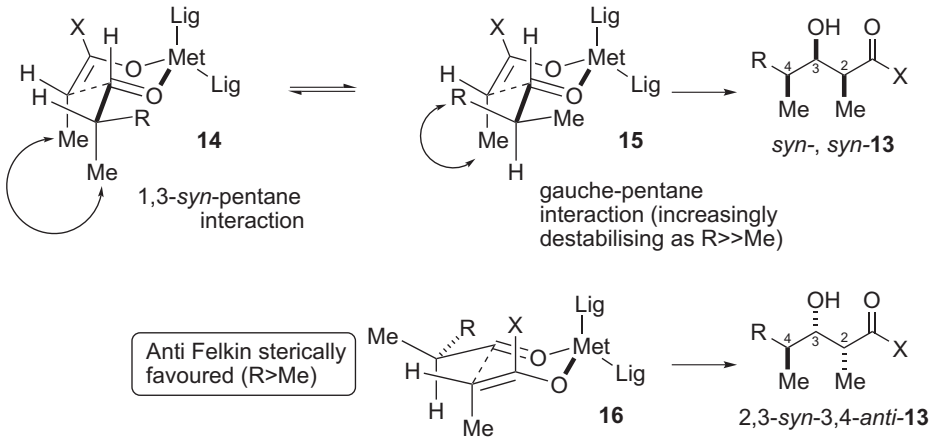

Transition States for *E*(O)-Enolate Aldol Reactions

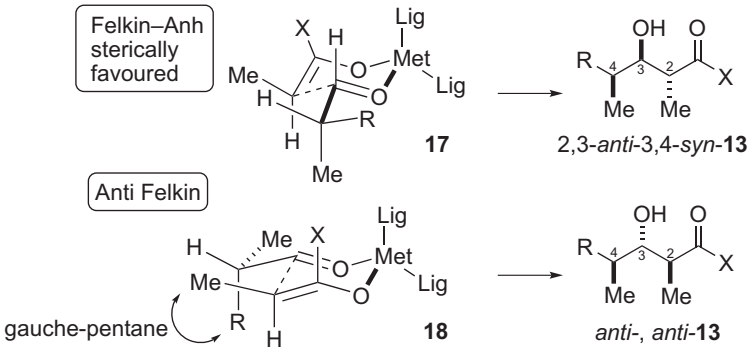

Scheme 8.

determined by acyclic stereocontrol. While reactions of *E*-enolates give the product predicted by the Felkin–Anh model, the opposite 'anti-Felkin' diastereomer is the major product of reaction of *Z*-enolates. According to Roush, the dominant stereocontrol element determining aldehyde diastereofacial selectivity is the minimisation of *gauche*-pentane interactions in the competing transition states. For *Z*-enolates, the Felkin–Anh transition state **14** contains an unfavourable *syn*-pentane interaction. A rotation of the aldehyde bond to the adjacent stereocentre of 120° partially relieves this interaction (transition state **15**), but this is still

destabilised relative to the anti-Felkin transition state **16** by a *gauche*-pentane interaction. The case for *E*-enolates is somewhat simpler, since the Felkin–Anh transition state **17** contains the fewest *gauche*-pentane interactions (cf. **18**) and also benefits stereoelectronically from the antiperiplanar alignment of the forming C–C and aldehyde C–R bonds. Hoffmann and Roush have reported similar diastereoselectivity patterns in allylation reactions.[13]

There have been recent reports of additions of nucleophiles to carbonyls adjacent to a polar stereocentre, where the stereoselectivity is also poorly rationalised by the polar Felkin–Anh model. Indeed, numerous authors have suggested that Cornforth-type transition states, where the polar substituent is orientated antiparallel to the carbonyl group, minimising dipolar interactions, might better explain such reactions.[14]

2.3. Recent evidence for Cornforth models

The dichotomy between Felkin–Anh and Cornforth transition states in the context of allylation reactions was investigated by Gung in 2001 using ab initio computational methods.[15] For the reaction of allylboronic acid **20** with 2-methoxypropanal **19**, the relative energies of the Felkin–Anh **22** and Cornforth **21** transition states (which both lead to the same product **23**) were calculated, with the former being higher in energy by 1.27 kcal/mol (Scheme 9). The criterion for the Felkin–Anh model, that the nucleophile approaches antiperiplanar to the αC–O, bond is poorly satisfied in this case. This deviation is attributed to conformational factors, particularly a *syn*-pentane interaction between the axial vinyl protons of the allylboron moiety and the α-methyl group of the aldehyde. In the light of these results the authors calculated the energies of individual fragments of the transition states with frozen geometry. However, they did not find any evidence of charge separation between the αC–O and carbonyl groups that would be expected for a Cornforth transition state. They concluded that the relative energies of the Felkin–Anh and Cornforth transition states were a function of conformational constraints only.

Cornforth transition-state models have found continued use in the study of diastereoselective allylation and crotylation reactions. In 2003, Batey reported the diastereoselective allylation and crotylation of α- and β-siloxy-substituted aldehydes under phase-transfer conditions, which was used in a total synthesis of tetrahydrolipstatin.[16] Both *E*- and *Z*-potassium allyl- and crotyltrifluoroborates **25** reacted with α-*tert*-butyldimethylsiloxy aldehydes **24** to give, in all but one case, the 2,3-*anti* product **26** in uniformly high yield (Scheme 10, Table 1).

The major product, 2,3-*anti*-**26**, was derived from a Cornforth transition state (**TS A**) for the reactions of *Z*-crotytrifluoroborates (entries 3 and 5), while the same product derived from a Felkin–Anh-type transition state (**TS C**) in the reactions of an *E*-crotyltrifluoroborate (entry 6) in agreement with the predictions of Roush.[11,13a] The analogous behaviour when R^3=Me was unexplained by the authors, but would suggest a greater *gauche*-pentane interaction between the allyl group and the aldehyde α-methyl moiety than between the allyl group and the α-siloxy substituent. A lower selectivity was observed in allylation reactions (entries 1 and 2), presumably resulting from less significant *syn*-pentane interactions in the transition state leading to 2,3-*syn*-**26** (**TS B**) (Scheme 11).

Detailed studies of Cornforth transition states for the aldol reaction combining experimental and computational data have been performed. However, experimental discrimination between Cornforth and polar Felkin–Anh models is difficult, particularly as both often predict the same product. An experiment that would differentiate between the two models was proposed by Evans.[17] As shown in the above examples of allylation and aldol reactions, such discrimination is possible when the nucleophile imposes a conformational constraint on the orientation of the stereocentre adjacent to the electrophilic carbonyl. For reactions of *E*- and *Z*-enolates,

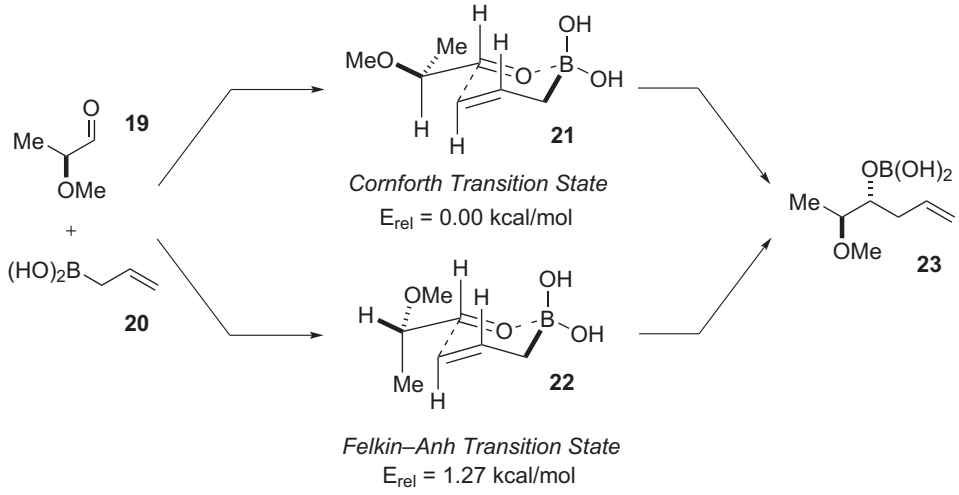

Scheme 9.

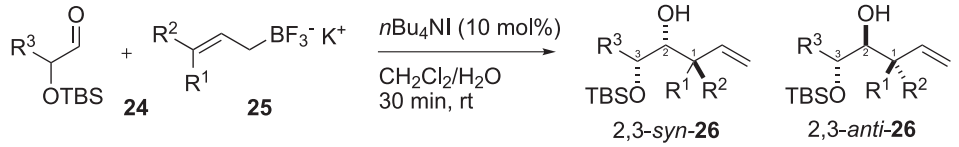

Scheme 10.

Table 1
Reaction of trifluoroborates **25** with aldehydes **24**

Entry	R^1	R^2	R^3	*E*/*Z*	Ratio of 2,3-*syn*/2,3-*anti* **26**	% Yield
1	H	H	Me	—	30:70	95
2	H	H	Ph	—	35:65	94
3	Me	H	Me	*Z*	5:95	95
4	H	Me	Me	*E*	75:25	95
5	Me	H	Ph	*Z*	10:90	97
6	H	Me	Ph	*E*	10:90	99

interaction. Therefore, *Z*-enolates are predicted to give superior 3,4-*anti* selectivity relative to *E*-enolates. Thus, the *E*- and *Z*-boron and lithium enolates of 2-methyl-3-pentanone **28** were combined with a representative set of α-oxy-substituted aldehydes **29** (Scheme 13, Table 2). In general, relative to *Z*-enolates, the *E*-isomers showed greatly diminished selectivity for the 3,4-*anti* diastereomer of **30**, in support of the Cornforth model.

More recently, Evans has performed a theoretical investigation of boron enolate addition to α-heteroatom-substituted aldehydes,

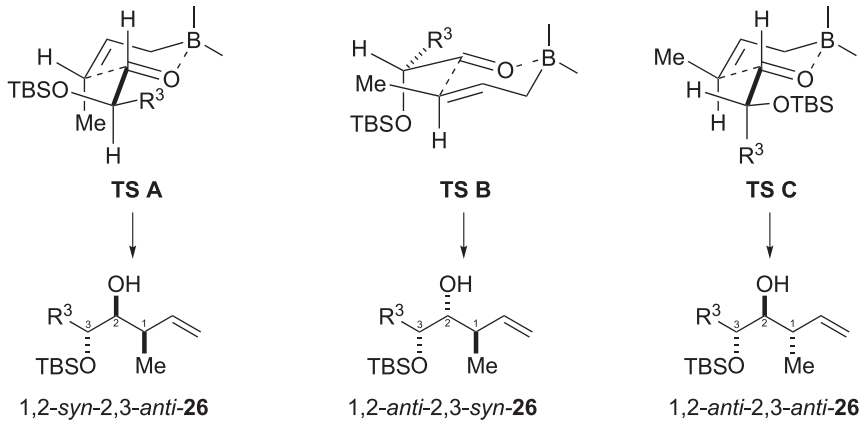

Scheme 11.

both Felkin–Anh and Cornforth transition states were proposed that lead to the 3,4-*anti* product **27**. The 2,3-relationship was set by the choice of *E*- or *Z*-boron enolate, the geometries of which are reliably reflected in the product stereochemistry. Lithium enolates were also included for generality, although they are inherently less diastereoselective (in defining the 2,3-relationship) (Scheme 12).

comparing polar Felkin–Anh and Cornforth transition-state models using DFT methods.[18,19] Highly electronegative substituents (F, OMe, Cl) and less electronegative substituents (PMe_2, SMe, NMe_2) were assessed. For the halopropanals **31** (X=F, Cl) transition states leading to both *anti*- (**TS A** and **C**) and *syn*-**32** (**TS B** and **D**) were calculated. For di- and tri-valent heteroatoms, where rotamers of the C–X bond

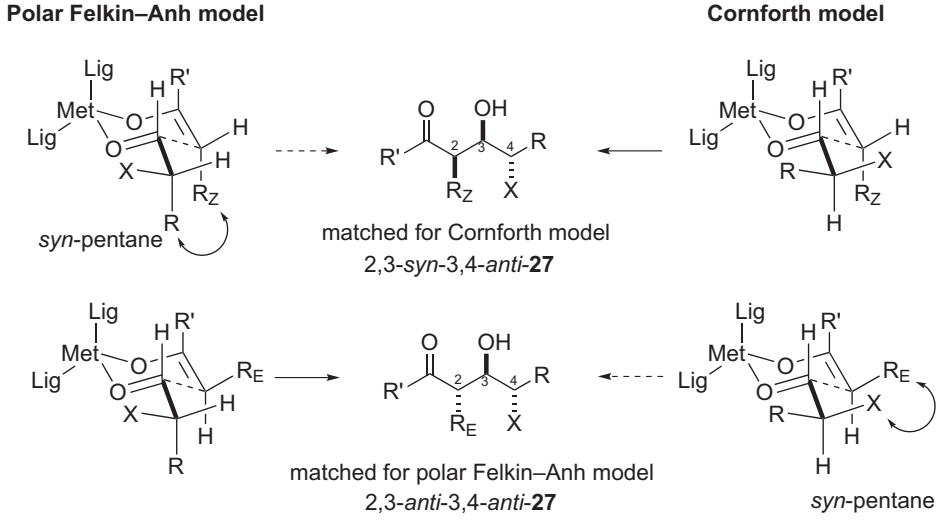

Scheme 12.

In the prediction of the polar Felkin–Anh model, the *Z*-enolate substituent causes a destabilising *syn*-pentane interaction, while the *E*-enolate substituent experiences no such interaction. Therefore, *E*-enolates are predicted to give superior 3,4-*anti* selectivity relative to *Z*-enolates. Conversely, in the prediction of the Cornforth model, the *E*-enolate substituent causes a destabilising *syn*-pentane interaction, while the *Z*-enolate substituent experiences no such

are possible, only the transition states leading to the *anti* product were calculated (Scheme 14, Table 3). The relative energies of Cornforth and Felkin–Anh transition-state structures are highly dependent on the nature of the heteroatom substituent, with chlorine, fluorine and oxygen substituents favouring the Cornforth arrangement and nitrogen, sulfur and phosphorus substituents favouring the polar Felkin–Anh arrangement.

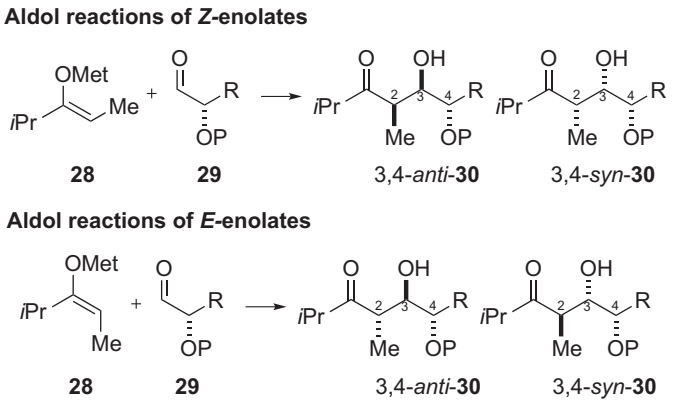

Scheme 13.

Table 2
Reaction of *E*- and *Z*-boron and lithium enolates of 2-methyl-3-pentanone **28** with α-oxy-substituted aldehydes **29**

Aldol reactions of *Z*-enolates					Aldol reactions of *E*-enolates				
Met	P	R	3,4-*anti*-/3,4-*syn*-**30**	% Yield	Met	P	R	3,4-*anti*-/3,4-*syn*-**30**	% Yield
9-BBN	Bn	Me	89:11	95	$(c\text{-Hex})_2$B	Bn	Me	33:67	59
9-BBN	Bn	*i*-Pr	98:2	73	$(c\text{-Hex})_2$B	Bn	*i*-Pr	67:33	77
9-BBN	TBS	Me	98:2	77	$(c\text{-Hex})_2$B	TBS	Me	21:79	77
9-BBN	TBS	*i*-Pr	98:2	72	$(c\text{-Hex})_2$B	TBS	*i*-Pr	43:57	85
Li	Bn	Me	89:11	67	Li	Bn	Me	93:7	92
Li	Bn	*i*-Pr	98:2	77	Li	Bn	*i*-Pr	80:20	78
Li	TBS	Me	95:5	65	Li	TBS	Me	85:15	78
Li	TBS	*i*-Pr	99:1	71	Li	TBS	*i*-Pr	88:12	80

Table 3
Relative energies of Cornforth and Felkin-Anh transition state structures

X		Cornforth		Polar Felkin–Anh	
		TS A	**TS B**	**TS C**	**TS D**
F	φ (deg)	166	196	264	76
	E_{rel}[a]	0.0	0.8	2.4	3.7
Cl	φ (deg)	175	186	267	76
	E_{rel}[a]	0.0	0.6	0.4	2.4
OMe	φ (deg)	171	—	267	—
	E_{rel}[a]	0.0	—	1.7	—
SMe	φ (deg)	174	—	271	—
	E_{rel}[a]	3.3	—	0	—
NMe_2	φ (deg)	172	—	272	—
	E_{rel}[a]	0.8	—	0.0	—
PMe_2	φ (deg)	175	—	276	—
	E_{rel}[a]	3.5	—	0.0	—

[a] Calculated using B3LYP method with 6-31G(d) basis set; energies in kcal/mol.

aldol reactions[17] in good agreement with experimental data. This work by Evans represents perhaps the most in-depth study in this area to date, and aspects of this methodology have been recently employed in the synthesis of the natural product, (+)-peluroside A.[20]

Similar relationships of Cornforth models with heteroatom electronegativity are evident in the investigations of Marco into doubly diastereoselective aldol reactions[21] of L-erythulose derivatives with aldehydes bearing an adjacent stereocentre.[22] In the most striking case, aldehydes bearing α-fluoro and α-benzyloxy groups **35** reacted via Cornforth transition states, while α-amino aldehydes **37** reacted via anti-Felkin–Anh transition states to give

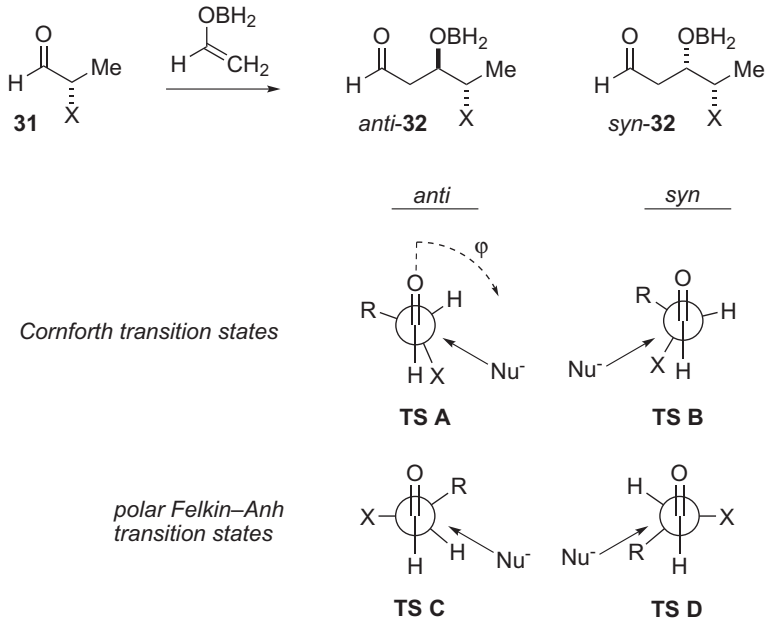

Scheme 14.

Further analysis suggested that the nucleophile→σ^*_{C-X} interaction central to the polar Felkin–Anh model was energetically insignificant in reactions of carbonyls with boron enolate nucleophiles. However, it was shown that, when X=SMe and X=PMe_2, perpendicular alignment of the C–X bond with the carbonyl group (as in the Felkin–Anh model) was favoured, due to $\sigma^*_{C-X}\rightarrow\pi^*_{C=O}$ delocalisation. Transition states were also calculated for the above **36** and **38**, respectively. In these cases, the non-stereogenic ketone **33** was used to form the corresponding *Z*-boron enolate **34**. Additional conformational constraints are placed on the transition states by the dipolar repulsion between the enolate C–O and remaining α C–OTBS bonds, resulting in an antiperiplanar alignment (Scheme 15). Aldehydes bearing α-methyl groups were also studied, which reacted via Felkin–Anh transition states as

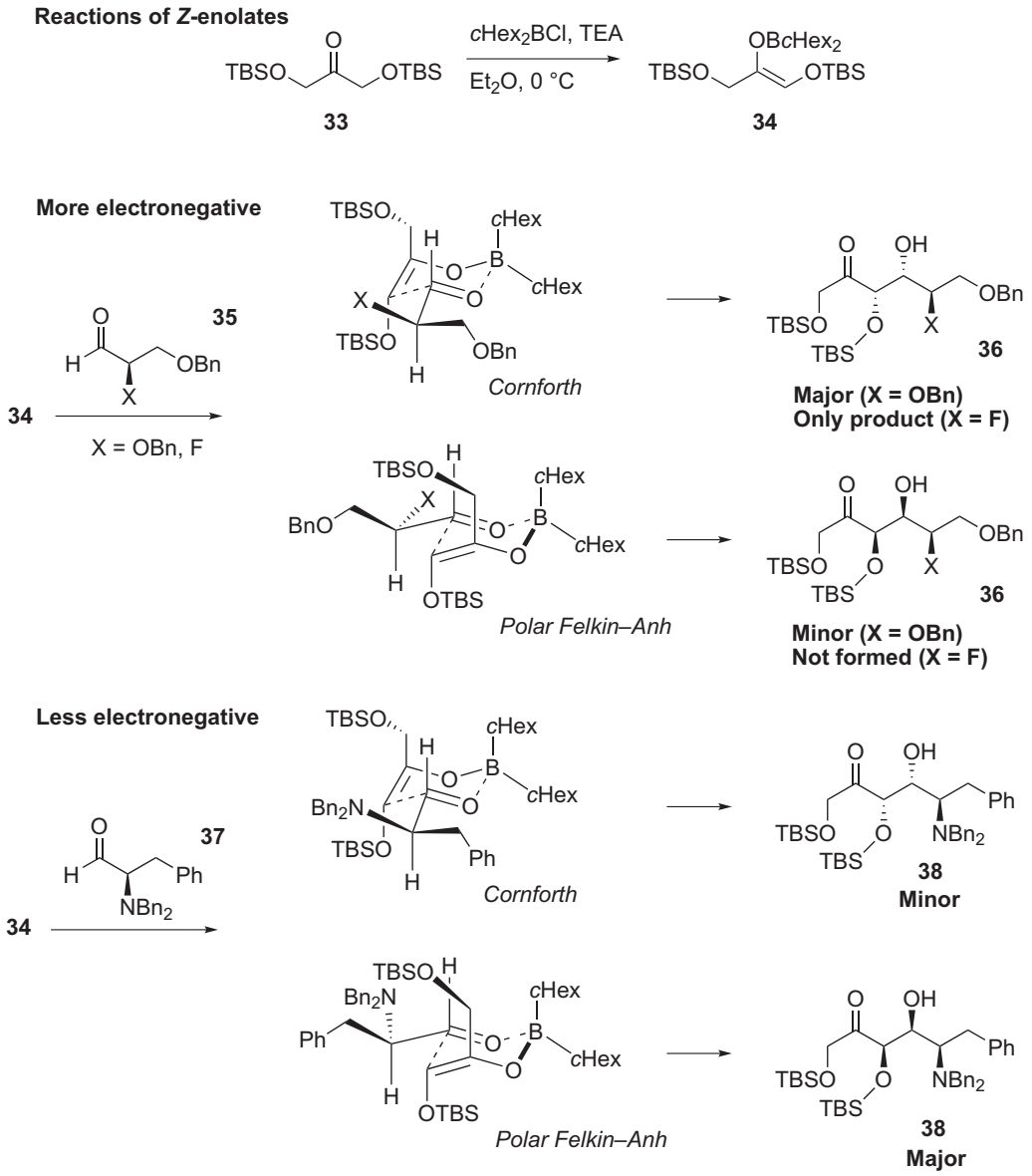

Scheme 15.

predicted, although computational investigations by other groups have recently suggested that Felkin–Anh models might not be as generally applicable for attack on carbonyls adjacent to non-heteroatomic stereocentres.[23]

2.4. Conclusions

Modelling of nucleophilic addition to carbonyls adjacent to a stereocentre is still a highly active area of development, with numerous studies over the last 10 years that challenge the dominance of the Felkin–Anh model.[24] Additional factors must be taken into account when the acyclic stereocontrol arises from the presence of stereocentres adjacent to well-defined transition states. In short, the rotational conformation around the α-stereocentre is dependent on the nature of the nucleophile. Additionally, although the Felkin–Anh model is still useful, its theoretical basis remains in question.[25] There is no one model that reliably describes all cases. However, in the case of polar stereocentres, there has been a resurgence in the use of the Cornforth model to describe diastereoselectivity.[26]

3. Addition to C=C double bonds with adjacent stereocentres

The case for addition of both nucleophiles and electrophiles to olefins is somewhat more complicated than for analogous reactions, with carbonyls. Felkin–Anh-type models provide a theoretical basis for these reactions where the carbonyl group is replaced by a C=C double bond (Scheme 16).[27] However, additional conformational constraints are imposed by the double-bond substituents and the level of acyclic stereocontrol is often highly dependent on the double-bond substitution pattern. This area has been reviewed relatively recently by both Reiser[4d] and Fleming[36]

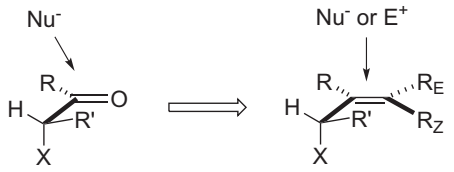

Scheme 16.

(vide infra). A brief historical treatment is given, followed by accounts of recent developments.

3.1. Electrophilic additions

Calculations of torsional effects in additions of electrophiles to substituted butenes by Houk suggested that staggered transition states were preferred in additions of electrophiles to C=C double bonds adjacent to a stereocentre.[28] Attack of the electrophile in these systems occurs perpendicular to the double bond; deviations from this trajectory suffered large energy penalties. Therefore, the lowest-energy structure is that in which the stereocentre exerts the least hindrance to the incoming electrophile, or, in an alternative view, that which interacts least with the forming bond. For hydroboration,[29] this corresponds to the staggered transition state **39** with the smaller (S) substituent pointing 'inside' the double bond, and attack *anti* to the L group. This conformation has the additional advantage of minimising 1,3-allylic strain. Notably, this corresponds to the *anti*-Felkin product **41**, derived from **40** as in the example of Kishi (Scheme 17).[30]

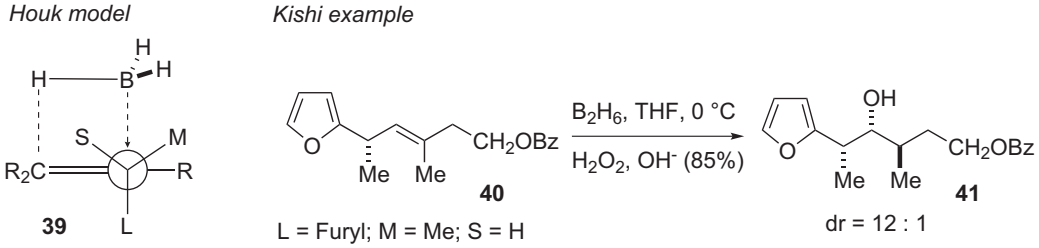

Scheme 17.

Kishi reported similar results in the osmylation of protected and unprotected allylic alcohols **42** to give **43** (Scheme 18, Table 4; showing selected examples).[31] The selectivity is rationalised by invoking the Houk model. The increased selectivity upon switching from *E*- to *Z*-allylic double-bond geometry is a clear indication of the importance of 1,3-allylic strain in this model. As will be seen, 1,3-allylic strain is perhaps the most important control element in additions to C=C double bonds, and is a component of most models. This subject has been reviewed in detail by Hoffmann.[32]

to C=C double bonds.[33] The OsO_4–TMEDA conditions, which exploit OH···O=Os hydrogen bonding,[34] were compared with the substoichiometric OsO_4–NMO 'Upjohn' conditions (Scheme 19, Table 5).

Transition states were proposed to account for these selectivity patterns (Scheme 20). The increase in magnitude of the observed *syn* selectivity on switching from *E*- to *Z*-isomers under Donohoe conditions is explained by **TS A** and **TS B**. In both, the hydrogen-bonding interaction is maintained that leads to attack of the oxidant from the same face as the alcohol. However, although **TS B**, which leads to the *anti* product, satisfies the conditions for hydrogen bonding, it is disfavoured by 1,3-allylic strain between the R and R_Z groups. Therefore, when the R_Z substituent is non-hydrogen, reaction via **TS A**, which leads to the *syn* product, is favoured. Similar transition states **TS C/D** can be proposed to account for the reversal in selectivity under Upjohn conditions. Although the selectivity is comparatively low under these conditions, the preferred *anti* products from the reaction of *E*-allylic alcohols can be formed via **TS C** in which the R group eclipses the double bond. Conversely, **TS D** must be invoked for oxidation of *Z*-allylic alcohols to minimise 1,3-allylic strain.[35]

This is defined by Fleming as the 'inside-methyl' effect[36] where, in systems lacking a significant 1,3-allylic strain component, the major product can arise from a transition state in which the smallest group does not eclipse the double bond (cf. **TS B/D**, Scheme 20). Its occurrence is highly dependent upon both the substrate and reaction in question. The effect is also observed in nucleophilic additions.

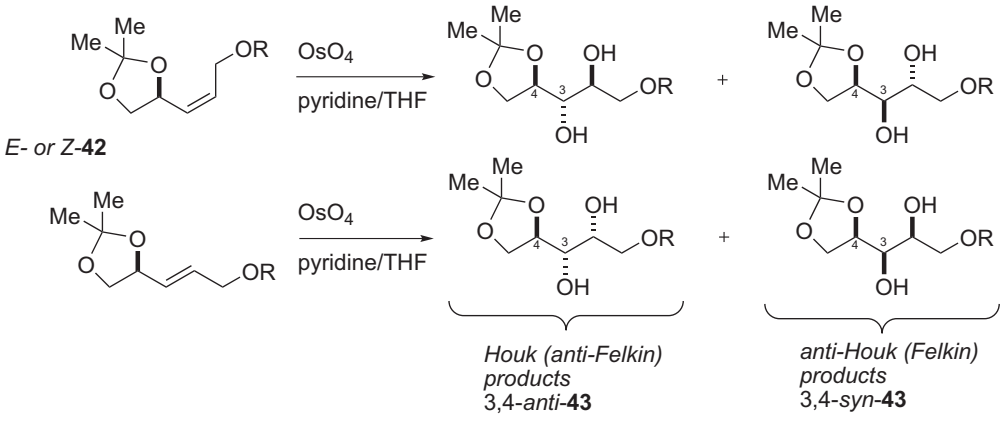

Scheme 18.

In a more recent example, Donohoe has reported that *syn* selectivity is possible in osmylations of unsaturated alcohols **44** to give **45** in the presence of TMEDA, which further illustrates the importance of 1,3-allylic strain for acyclic stereocontrol in additions

3.2. Nucleophilic additions

The majority of studies in this area have concentrated on the conjugate addition of organocuprate nucleophiles to enoates **46**

Table 4
Osmylation of allylic alcohols **42**

Entry	R	*E*/*Z*	Ratio 3,4-*anti*-/3,4-*syn*-**43**
1	H	*E*	3.3:1
2	C(O)^{t}Bu	*E*	4.2:1
3	TBDPS	*E*	3.1:1
4	H	*Z*	6.1:1
5	C(O)^{t}Bu	*Z*	6.3:1
6	TBDPS	*Z*	8.0:1

(Scheme 21). Yamamoto argued that the reactive conformation is stabilised by overlap of the electron-rich C–R bond with the developing C–Nu σ* orbital. The model correctly predicts a reversal from *anti* to *syn* selectivity in the reactions of *Z*-enoates, as increased 1,3-allylic strain favours the conformation with the hydrogen roughly eclipsing the double bond.

Kornienko studied the addition of various diarylcuprates[43] to a representative set of γ-alkoxyenolates **48** to give **49**, with variations in the alkoxy group, R group and enolate geometry (Scheme 22, Table 6). The high selectivities in additions to *E*-enoates are consistent with the modified Felkin–Anh model, as the selectivity is independent of the size of the R′ group (entries 1 and 2), which is orientated antiperiplanar to the incoming nucleophile. The reduction in selectivity with reducing size of the R group is also consistent with this model (entries 2, 3 and 4). The Yamamoto model leads to the opposite prediction that selectivity should be highly dependent on the size of the R′ group (OR′ eclipses the enoate in the transition state, leading to the *anti* product) and that selectivity should be largely independent of the R group. The moderate selectivities for addition to *Z*-enoates are poorly explained by both models. The modified Felkin–Anh model suggests *anti* selectivity should be higher for *Z*-enoates, while the Yamamoto model suggests that *syn* products should predominate.

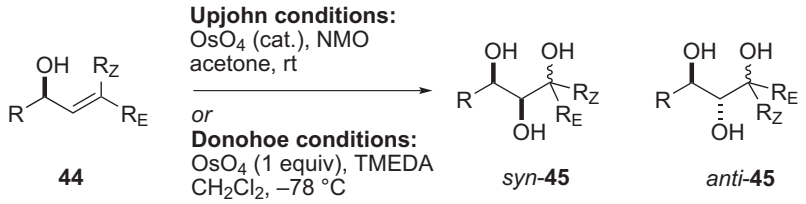

Scheme 19.

Table 5
Comparison of Upjohn and Donohoe dihydroxylation conditions

Entry	R	R_E	R_Z	Upjohn conditions		Donohoe conditions	
				Ratio *syn*-/*anti*-**45**	% Yield	Ratio *syn*-/*anti*-**45**	% Yield
1	*n*-Pr	H	H	25:75	80	60:40	74
2	*n*-Pr	*n*-Pr	H	25:75	85	75:25	83
3	*n*-Pr	*t*-Bu	H	17:83	83	80:20	75
4	*i*-Pr	*n*-Pr	H	20:80	75	75:25	84
5	*n*-Pr	H	*n*-Pr	62:38	76	96:4	74
6	*t*-Bu	H	*n*-Pr	80:20	85	96:4	79
7	*n*-Bu	Me	Me	66:34	96	96:4	78

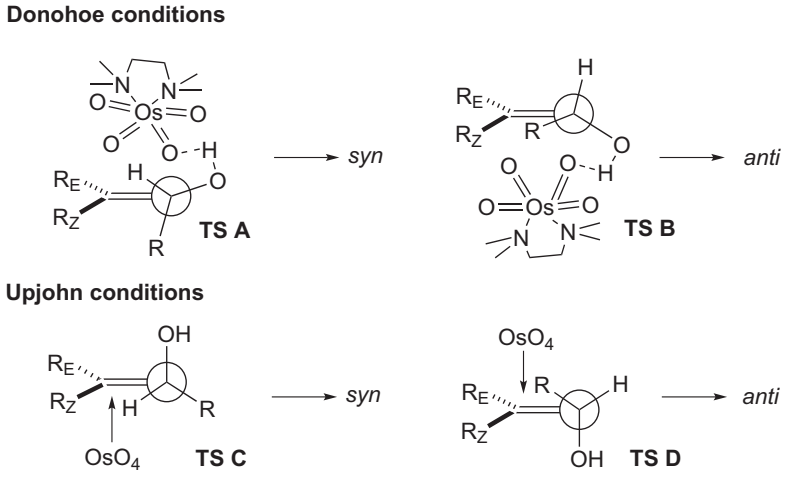

Scheme 20.

bearing a γ-stereocentre, in particular due to the use of this method in the synthesis of polypropionate building blocks for natural products.[37] A summary of models for describing this reaction has recently been published by Kornienko.[38] In the case of γ-alkoxy and γ-siloxy stereocentres, the *anti* product *anti*-**47** generally predominates.[39] The two most prevalent models for this selectivity are the 'modified Felkin–Anh' originally described by Roush,[40] which parallels that for electrophilic addition to C=C double bonds, and the Yamamoto model,[41] which has many features in common with the Cieplak[42] and Houk 'inside-alkoxy'[57] models vide infra

A revised model was suggested that takes into account recent mechanistic studies in the conjugate additions of organocuprates,[44] with the assumption that the reductive elimination step of the reaction is both rate- and stereochemistry-determining. This contrasts with the Yamamoto and modified Felkin–Anh models, which assume complexation with the enoate to be the step controlling facial selectivity (Scheme 23).

Both Felkin–Anh and Yamamoto transition states for the reductive elimination step contain eclipsing interactions with the complexed and almost planar organocuprate. The transition states

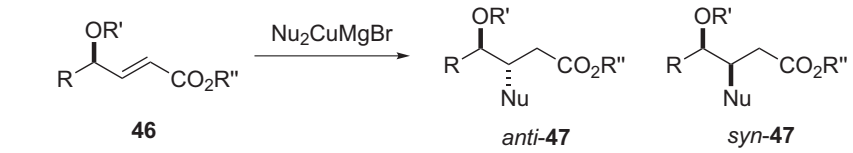

Modified Felkin–Anh model:

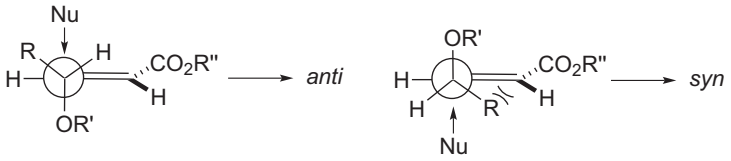

Yamamoto model:

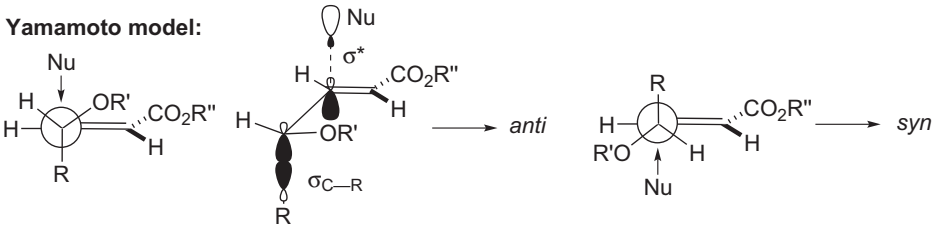

Scheme 21.

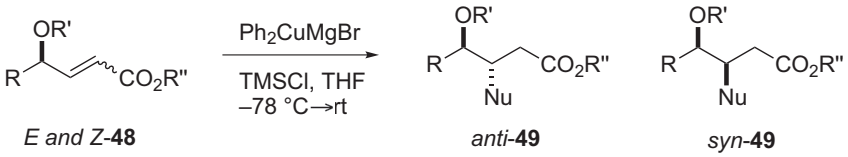

Scheme 22.

Table 6
Addition of diarylcuprates **43** to γ-alkoxyenolates **48**

Entry	R	R′	R″	*E*/*Z*	% Yield	Ratio *anti*-/*syn*-**49**
1	$CH_2OTBDPS$	MOM	Et	*E*	80	>50:1
2	$CH_2OTBDPS$	Bn	Me	*E*	88	>50:1
3	CH_2OBn	Bn	Me	*E*	94	14.6:1
4	Me	Bn	Me	*E*	89	5.4:1
5	$CH_2OTBDPS$	Bn	Me	*Z*	87	1.6:1
6	CH_2OBn	Bn	Me	*Z*	72	2.8:1
7	Me	Bn	Me	*Z*	65	3.4:1

proposed by Kornienko position the R and OR′ groups away from the large cuprate moiety.[45] Additionally notable are the two roughly antiperiplanar relationships in this transition state, firstly between the C_γ–OR′ and forming C_β–Ar bonds and, secondly, between the C_γ–R and breaking C_β–Cu bonds. In the former, favourable mixing of the $\sigma_{C\beta-Ar}$ and low-lying $\sigma^*_{C\gamma-OR'}$ orbitals is maintained, while, in the latter case, overlap of the electron-rich $\sigma_{C\gamma-R}$ and $\sigma^*_{C\beta-Cu}$ orbitals assists the departure of copper. These transition states are consistent with the experimental data.

The sense of selectivity is reversed in the presence of γ-amino stereocentres, and the *syn* product predominates. This stereochemical divergence was discussed as early as 1991 by Hanessian.[46] Two substrates **50**, derived from Garner's aldehyde,[47] and **52** underwent *syn*-selective addition with dimethylcuprate–TMSCl (Scheme 24). According to Hanessian, the *syn*-products **51** and **53** could derive from either Felkin–Anh or Yamamoto transition states, although neither of these give a convincing explanation of the reversal of selectivity in changing from oxygen to nitrogen.

A more recent treatment of this dichotomy has been given by Kornienko.[48] Substrates **54** and **50**, similar to those investigated by Hanessian, were treated with a variety of diarylcuprates (Scheme 25, Table 7) to give **55** and **56**, respectively. Although diastereoselectivity was effectively absolute in all cases, much lower yields were observed for the bulkier substrate **54**.

In common with the previous study, considering that the Felkin–Anh model predicts predominance of the *anti* product, a 'reductive–elimination' transition state was proposed to account for the observed *syn* selectivity (Scheme 26). Although the reduced yields in the case of bulkier R groups (increased 1,3-allylic strain) agree with this model, it is unclear whether this transition state benefits from the favourable orbital interactions of the transition state leading to the *anti* product.

In additions of organocuprates to C=C double bonds adjacent to a silicon-containing stereocentre, diastereoselectivity is somewhat lower. Fleming reported the 1,4-addition of silylcuprates to enoates **57**, with silicon stereocentres at either the α- or β-position, to give esters **58**.[49] Attack occurred predominantly *syn* to the silicon substituent, with the hydrogen eclipsing the double bond. It is difficult to rationalise this result using the above reductive elimination transition states, although it may be consistent with a Yamamoto-type model in which the *anti* product is disfavoured by the silicon group roughly eclipsing the double bond (Scheme 27).

Further recent examples of acyclic stereocontrol in organocuprate additions have been reported by Breit, who used phosphine substituents for directed delivery of the cuprate.[50] While *E*-configured substrates *E*-**61** afforded *anti*-**62**, the *syn* products were obtained from the isomeric *Z*-configured substrates *Z*-**61**. The level

Mechanism of cuprate addition:

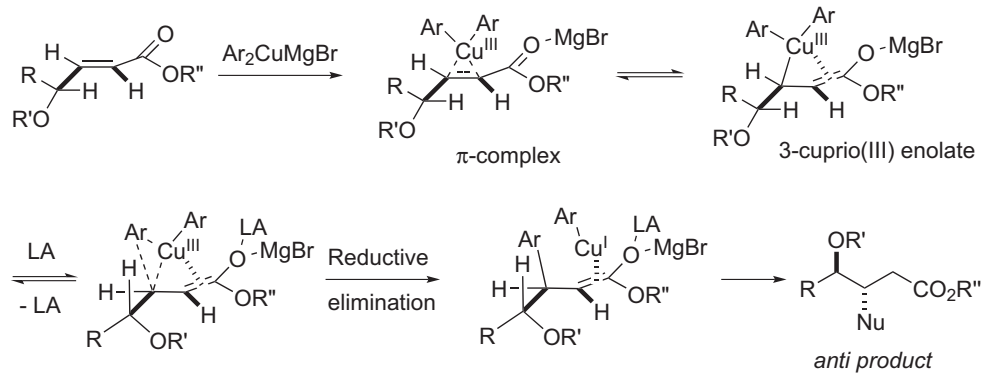

Reductive elimination transition states:

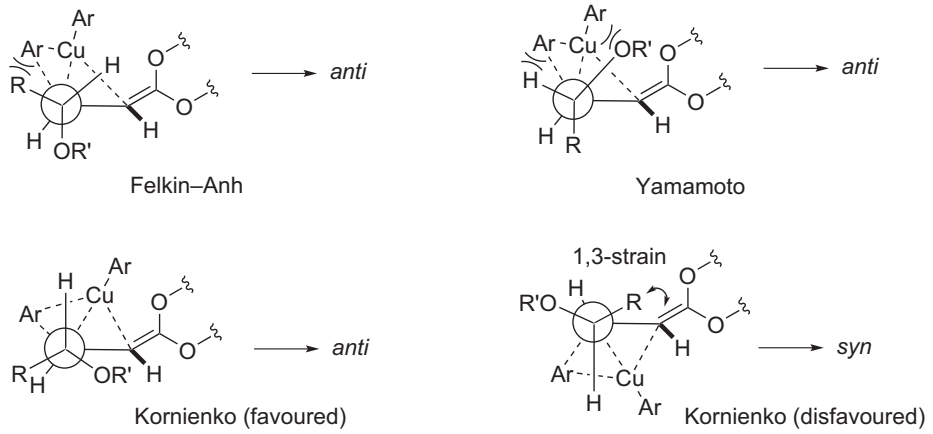

Scheme 23.

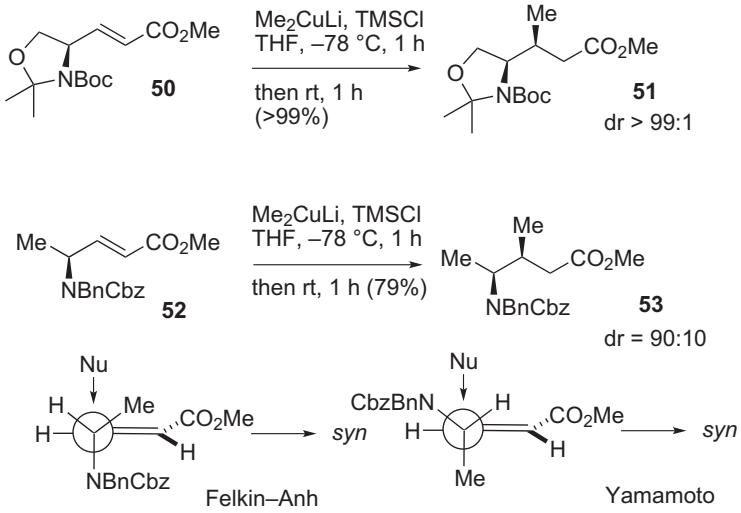

Scheme 24.

of selectivity was independent of the size of the nucleophile (Scheme 28).

Carbon nucleophiles undergo stereoselective addition to enoates with a γ-stereocentre, and similar models have been used to explain these reactions. The sense of addition of lithium amides varies between *syn* and *anti*, depending on the substrate,[51,52] while hydroxylamine nucleophiles generally give the *syn* product.[53] Alkoxide nucleophiles have also been studied.[54] The *anti* sense of rhodium-catalysed conjugate addition of boronic acids to γ,δ-alkoxy enoates has been recently explained using a reductive elimination model.[55]

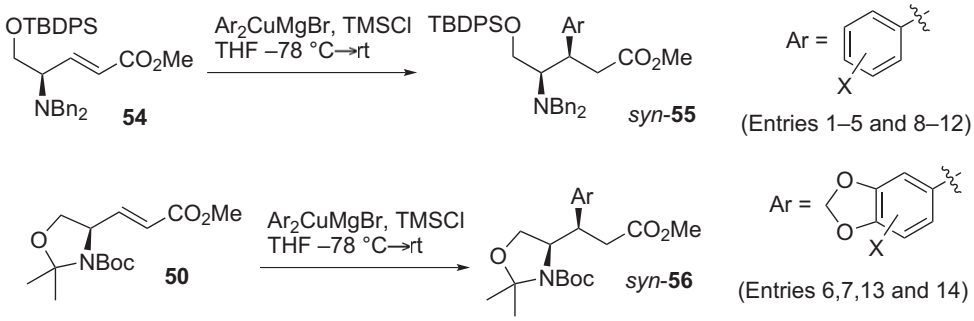

Scheme 25.

Table 7
Addition of diarylcuprates to **55** and **50**

Reaction of **54**				Reaction of **50**			
Entry	X	Yield (%)	Ratio *syn*-/*anti*-**55**	Entry	X	Yield (%)	Ratio *syn*-/*anti*-**56**
1	H	58	>20:1	8	H	95	>20:1
2	4-OMe	50	>20:1	9	4-OMe	87	>20:1
3	4-F	55	>20:1	10	4-F	92	>20:1
4	4-Cl	58	>20:1	11	4-Cl	83	>20:1
5	3,4-OMe	49	>20:1	12	3,4-OMe	70	>20:1
6	H	52	>20:1	13	H	92	>20:1
7	5-OMe	0	—	14	5-OMe	70	>20:1

conclusive explanations for the changing sense of selectivity with changing γ-heteroatom. Above all, 1,3-allylic strain dominates as an essential control element.

4. Pericyclic reactions

4.1. [3+2] Cycloadditions

Models for [3+2] cycloadditions follow naturally from those for addition to C=C double bonds, although they differ significantly from Felkin–Anh-type models. The case for 1,3-dipolar addition to

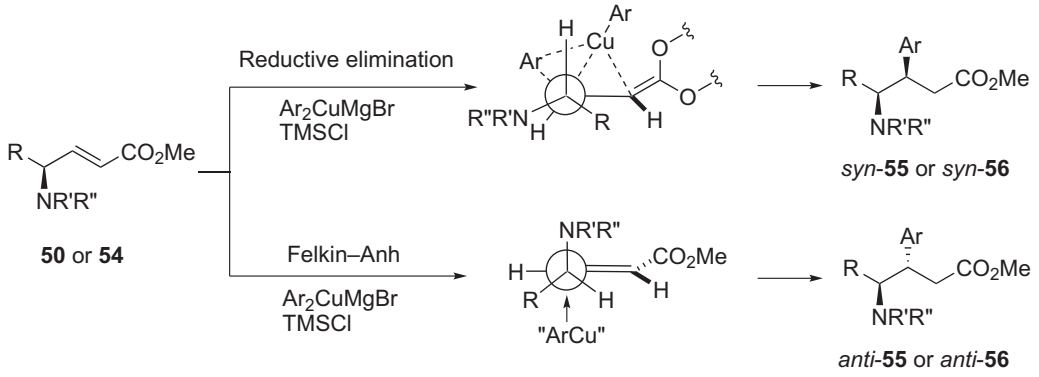

Scheme 26.

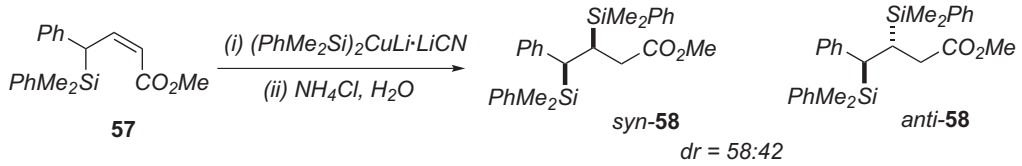

Scheme 27.

3.3. Conclusions

Compared to the analogous reactions of carbonyls, addition to double bonds adjacent to a stereocentre is less well defined. Although the Houk model correctly predicts the results of electrophilic addition in many cases, there are exceptions in which the major product arises from seemingly hindered transition states (cf. the inside-methyl effect). For nucleophilic additions, in particular 1,4-addition to enoates with γ-stereocentres, the sense of diastereoselectivity follows clear trends. However, neither the modified Felkin–Anh, Yamamoto or reductive elimination models give a C=C double bond adjacent to a stereocentre has been extensively investigated, particularly for chiral allyl ethers **63**. This area has been most recently reviewed in 2001, in which the authors highlight the accuracy with which the established theories predict the observed stereoselectivity.[56] The two key factors at work are 1,3-allylic strain and the 'inside-alkoxy' effects first postulated by Houk (Scheme 29).[57]

Houk calculated the relative energies of methyl and methoxy substituents at each of the staggered positions in the cycloaddition transition state. The methyl group preferentially adopted the *anti* configuration, avoiding the *inside* conformation on steric

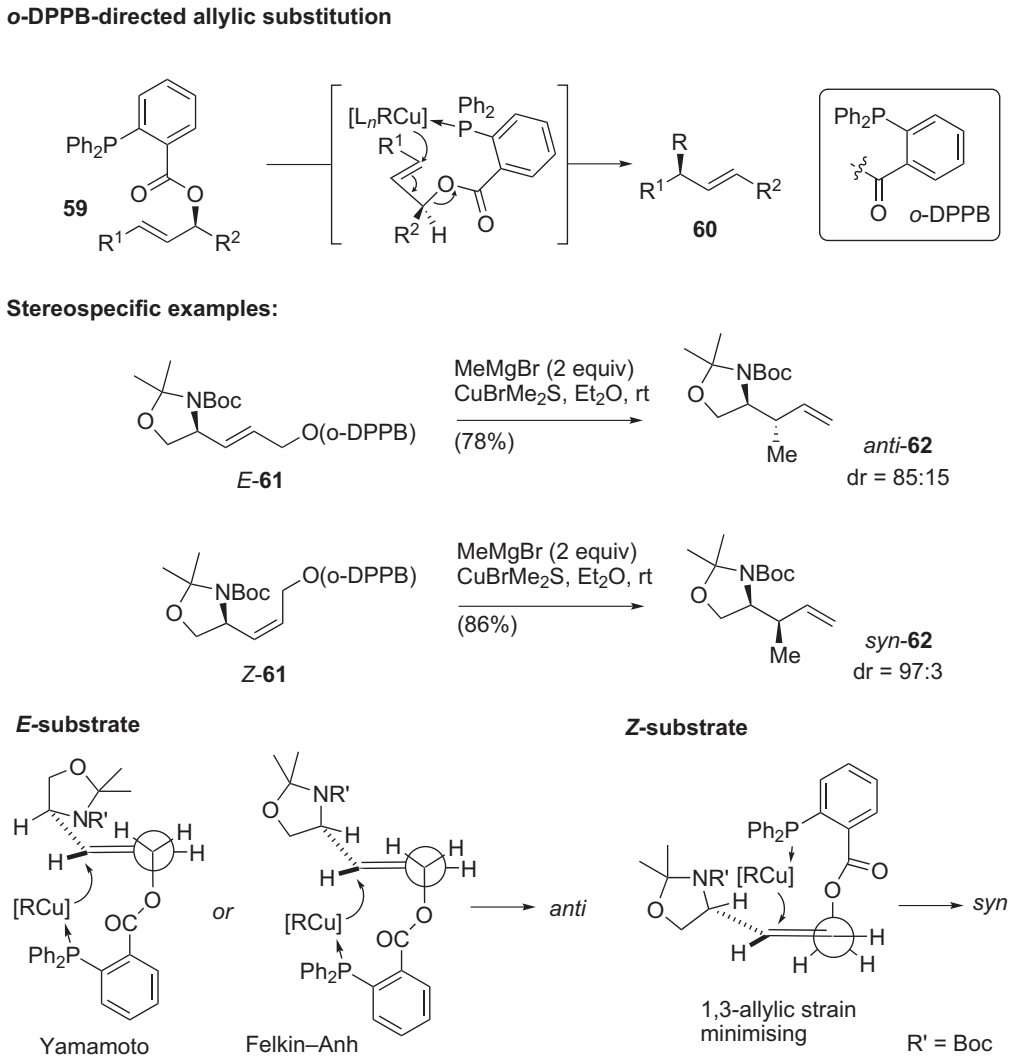

Scheme 28.

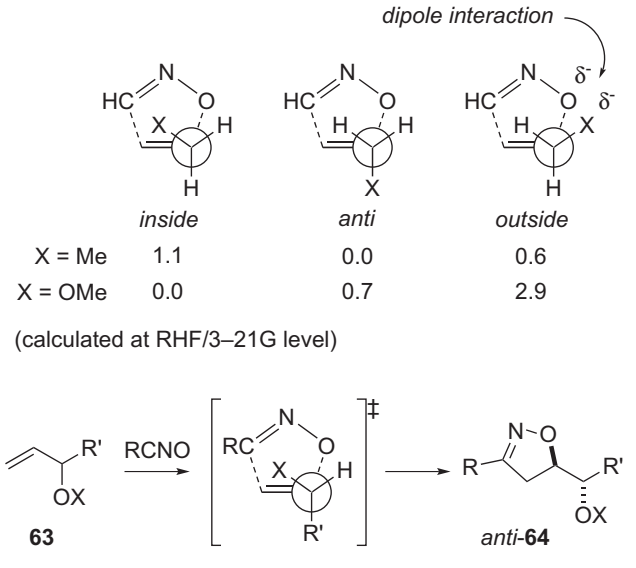

Scheme 29.

grounds, and allowing hyperconjugation of the σ_{C-Me} and electron-deficient $\pi^*_{C=C}$ bonds. The methoxy group was situated *inside* in the lowest-energy transition state. In the *anti* OMe position, overlap between the $\pi_{C=C}$ and σ^*_{C-O} orbitals removes electron density from the reacting olefin, disfavouring this transition state. Notably, the *anti* disposition of alkoxy groups relative to reacting olefins is shown to be a stabilising interaction in other pericyclic reactions, particularly sigmatropic rearrangements, due to a $\pi^*_{C=C}/\sigma^*_{C-O}$ interaction. Overall, the most unfavourable orientation is OMe *outside*, which is electrostatically destabilised by interaction of the partial negative charges of the approaching oxygen atoms.

In the case of *Z*-configured substrates where 1,3-allylic strain is greater, the alkoxy group adopts the *anti* position, with the smallest substituent lying *inside*. An example of this is shown in the intramolecular cycloaddition of *Z*-allylic ether **65** (Scheme 30).[58] Two possible allylic strain-minimising conformations are possible, yet the *outside* alkoxy/*anti* methyl transition state leading to *syn*-**66** is electrostatically disfavoured.

In contrast to the examples shown above of conjugate nucleophilic addition to enoates, alteration of the heteroatom causes little variation in the sense of the selectivity, although some exceptions have been reported. Cycloadditions of nitrile oxides with allylic isoxazoles **67** occur in the inside alkoxy sense and the *anti* product

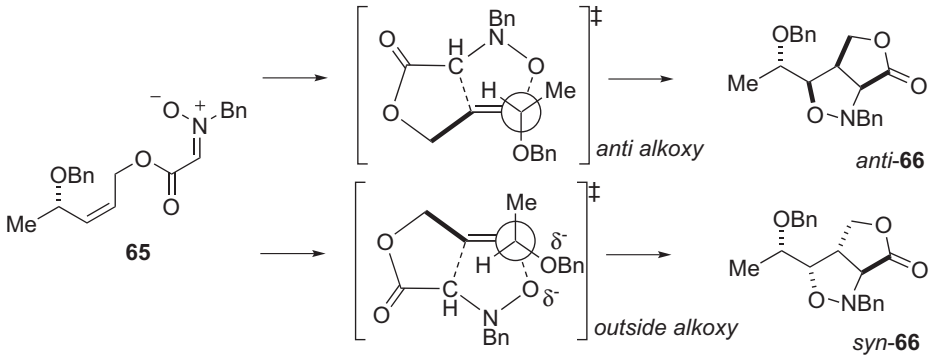

Scheme 30.

68 predominates (Scheme 31).[59] Selectivities are slightly lower than those for allylic ethers, which correlates with the lower electronegativity of nitrogen, causing less destabilisation in *anti* and *outside* transition states. Selectivities for the *anti* product are lower still for acyclic allylic amines.[59a,60]

More recently, the preferred conformations of allylic fluorides in transition states for their nitrile oxide cycloadditions have been studied and compared with experimental data.[61] Allylic fluorides were found to react in the sense predicted by the inside-alkoxy model, with fluorine taking the place of the alkoxy substituent.[62] Three allylic fluorides **69**, **71** and **74** were treated with propionitrile oxide to give the corresponding cycloadducts (Scheme 32). Allylic fluoride **69** reacted in favour of the adduct *anti*-**70**. Reaction of **71** and **74** both afforded mixtures of regio- and stereoisomers.

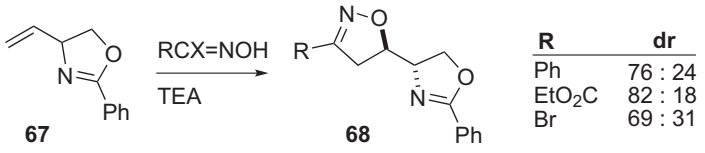

Scheme 31.

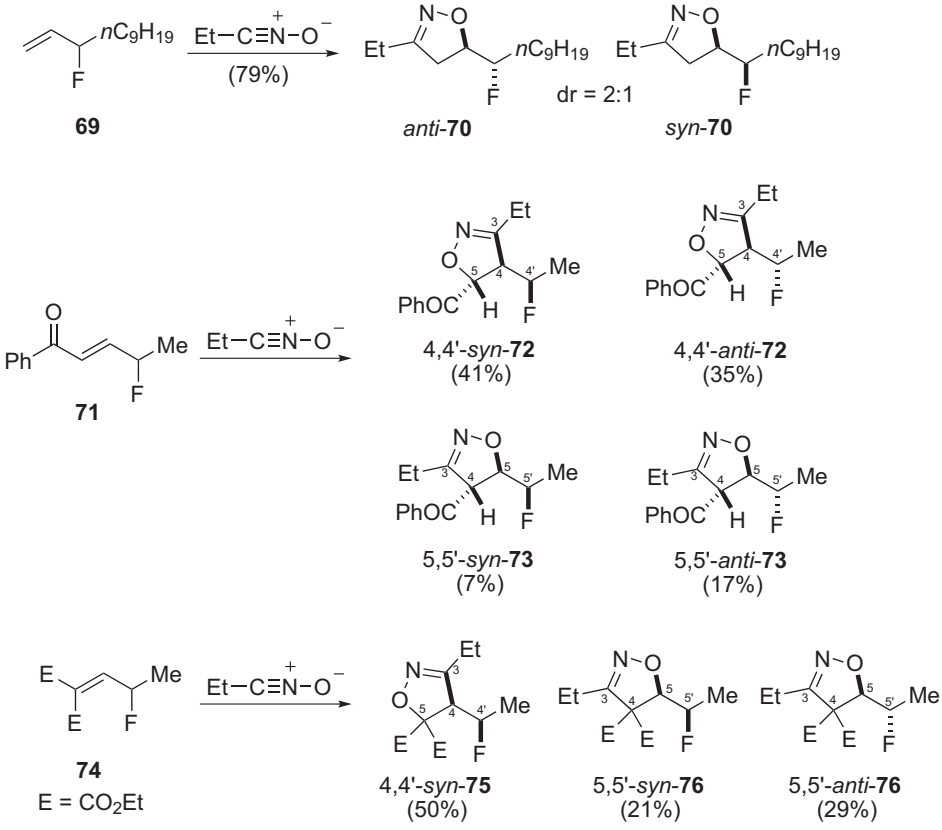

Scheme 32.

For **71** in the series with the stereocentre at the isoxazole 4 position (**72**), there was a slight preference for the *syn* cycloadduct. For the series with the stereocentre at the isoxazole 5 position (**73**) (in common with the above examples), a distinct preference for the *anti* cycloadduct was observed. For **74** in the series with the stereocentre at the isoxazole 4 position (**75**), only the *syn* cycloadduct was observed, while, with the stereocentre at the 5 position (**76**), there was a slight bias for the *anti* product.

These observations were explained using transition state searches (Scheme 33, calculated at the B3LYP/6-31G* level). For the 5-substituted regioisomer, the lowest-energy transition state (**A**) has fluorine *inside*, with the methyl group in the *anti* position. The second-lowest transition state (**D**), which leads to the *syn* product also has fluorine *inside*, but, in this case, methyl is *outside* and overlaps poorly with the double bond. However, for transition states leading to the 4-substituted regioisomer, an *inside* fluorine is destabilising, due to electrostatic interactions with the oxygen of the 1,3-dipole (transition states **G** and **J**), and the sense of selectivity is reversed. The lowest-energy transition state, from which the *syn* product is formed (**K**) has fluorine *outside*, pointing away from the 1,3-dipole and methyl *anti* in good overlap with the dipolarophile double bond. These transition states are in good agreement with the above data.

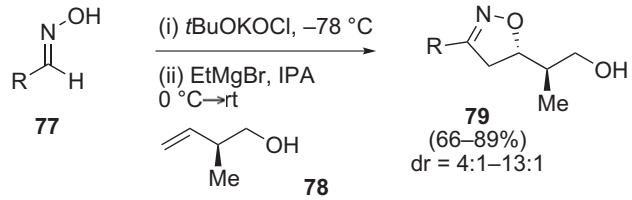

Scheme 34.

Houk has proposed transition states to account for this selectivity, which are based on the inside-alkoxy model (Scheme 35).[64] Reactions with and without a chelating magnesium atom between the two oxygens were compared. For both, the lowest-energy transition state had the alcohol in the *outside* position and the methyl group *anti*. This leads to the *anti* isoxazole product, as observed. In the non-chelation case, a hydrogen-bonding interaction between the 1,3-dipole oxygen and the homoallylic alcohol was observed. The next-lowest transition state, which leads to the *syn* product was destabilised by 1 kcal/mol. For the chelated transition state, the lowest *syn* transition state was destabilised relative to the lowest-energy *anti* transition state by 3 kcal/mol,

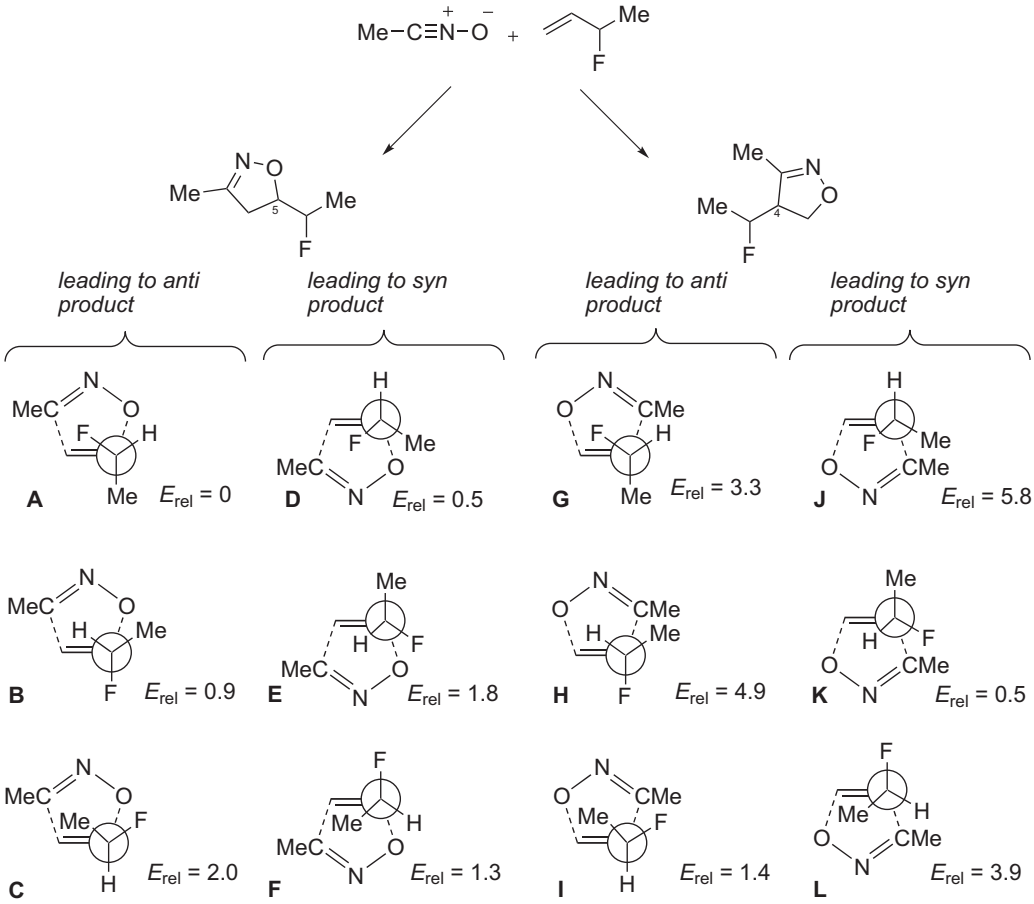

Scheme 33.

Progress has also been made in the study of 1,3-dipolar cycloadditions of homoallylic alcohols. Carreira has recently shown good *anti* selectivity for cycloaddition of nitrile oxides derived from oximes **77** with homoallylic alcohol **78** to give **79** in the presence of a metal counterion (Scheme 34).[63]

consistent with the observed selectivities. Conformations placing the magnesium ether in an *inside* arrangement were further destabilised by around 7–8 kcal/mol. For both cases, hydrogen bonding or chelation withdraw electron density from the 1,3-dipole, contributing to electron deficiency in the transition state.

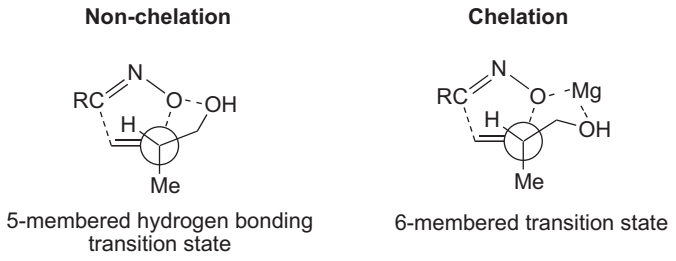

Scheme 35.

Thus, it is important that the methyl group lies in the *anti* position, in hyperconjugation with the olefin, which is even more electron deficient in this reaction compared to cycloadditions of chiral allylic ethers. Similar chelation models have been reported for allylic alcohol substrates.[65]

Only a very small section of the literature on [3+2] cycloadditions has been discussed here, and acyclic stereocontrol is certainly not limited to nitrile oxide additions to olefins with adjacent stereocentres. There are many other examples of diastereoselective [3+2] cycloadditions that are beyond the scope of this review. As a representative example, Padwa has reported acyclic stereocontrol in the rhodium-catalysed [3+2] cycloaddition of isomünchone dipoles with a variety of dipolarophiles derived from **80**, to give **82** (Scheme 36).[66] The conformation of the acyclic amide substituent of **81** determined the sense of diastereoselectivity,[67] with the hydrogen eclipsing the oxonium of the 1,3-dipole to minimise 1,3-allylic strain. Attack of the electrophilic dipolarophile occurred on the most electron-rich face of the 1,3-dipole. This effect, discussed by Kahn and Hehre,[68] is also observed in [4+2] cycloadditions.

4.2. [4+2] Cycloadditions

Similarly well investigated and modelled are [4+2] cycloadditions, particularly the Diels–Alder and hetero-Diels–Alder reactions.[69] Electrostatic interactions between the diene and dienophile have been shown to play an important role (cf. Scheme 36). Diels–Alder reactions of electron-rich dienes and electron-poor dienophiles should occur preferentially onto the more nucleophilic diene face, and onto the face of the dienophile, which exhibits greater electrophilicity (Scheme 37).[68]

Houk has suggested an inside alkoxy-type effect (which has an electrostatic component) to explain the stereoselective reactions of chiral allylic alcohols and ethers **83** with highly electron-deficient hexachlorocyclopentadiene **84**, which is in good agreement with experimental data.[70] In the analogous sense to [3+2] cycloadditions of nitrile oxides with chiral allylic ethers, the alkoxy group lies *inside*, avoiding electrostatic interactions with chlorine, while the alkyl group prefers an *anti* alignment with the olefin (Scheme 38).

Like [3+2] cycloaddition reactions of nitrile oxides with chiral allylic fluorides, Diels–Alder reactions of chiral allylic fluorides can be described by the inside-alkoxy model. Grée et al. studied the Diels–Alder reactions of allylic fluorides **86** with 2,3-dimethyl-1,3-butadiene **87** to give **88** and **88′** (Scheme 39, Table 8).[71] Where observed (entries 2 and 3), selectivities were in the inside fluorine sense. The reaction was unselective when a nitrile substrate was used (entry 1).

Acyclic stereocontrol in the intramolecular Diels–Alder (IMDA) reaction has also seen recent interest. The reaction can be controlled by stereocentres adjacent to the dienophile moiety. Sherburn studied the IMDA reactions of various ascorbate-derived substrates **89** to give **90a–d**.[72] The level of selectivity varied greatly

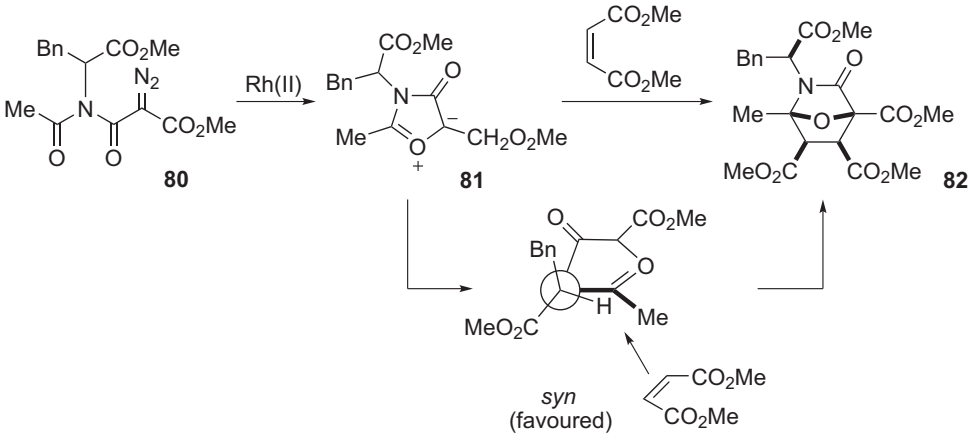

Scheme 36.

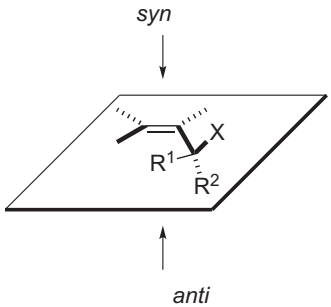

	Electrophile	Nucleophile
X = electron rich	syn	anti
X = electron poor	anti	syn

Scheme 37.

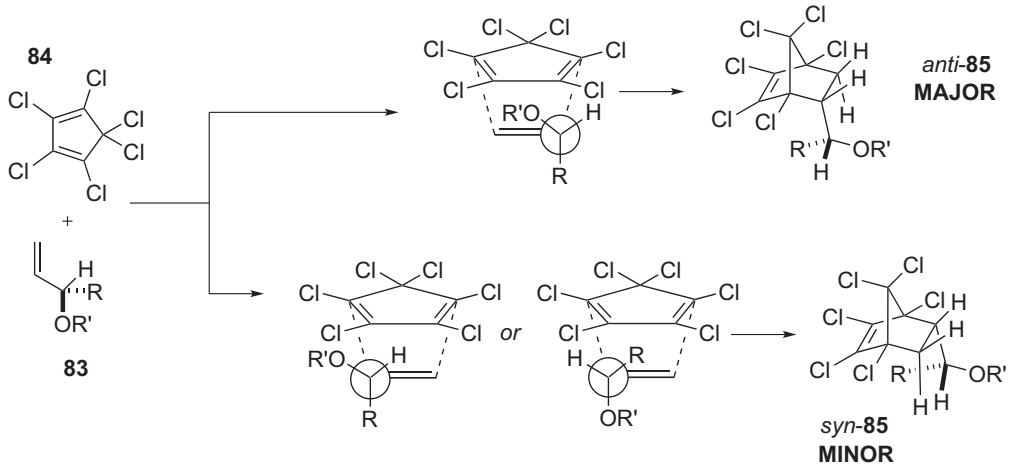

Scheme 38.

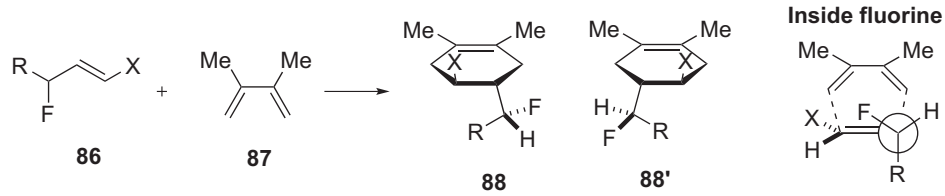

Scheme 39.

Table 8
Diels–Alder reactions of allylic fluorides **86** with 2,3-dimethyl-1,3-butadiene **87**

Entry	R	X	% Yield	Ratio **88**/**88′**
1	Me	CN	40	50:50
2	Me	COPh	85	76:24
3	*t*-Bu	COPh	90	81:19

with the group P. Based on computational studies, a model was proposed to account for these selectivities, which is in agreement with both the inside alkoxy and Kahn/Hehre models (Scheme 40, Table 9).

4.3. [3,3]-Sigmatropic rearrangements

Acyclic stereocontrol in [3,3]-sigmatropic rearrangements has typically been studied in the context of the Claisen rearrangement. In a generic ketene acetal Claisen precursor **91** (Scheme 41), 1,2-induction of the newly formed C1–C6 bond of **92** via acyclic stereocontrol is possible when stereocentres are positioned adjacent to the C1 and C5-6 positions. This area has been previously reviewed in the context of the Ireland–Claisen rearrangement,[3] and asymmetric [3,3]-sigmatropic rearrangements.[73] During rearrangement, C4 becomes, and C5 remains, sp^2-hybridised and, although stereocentres adjacent to these positions can affect stereochemistry in a similar sense,[74] it is beyond the scope of this review.

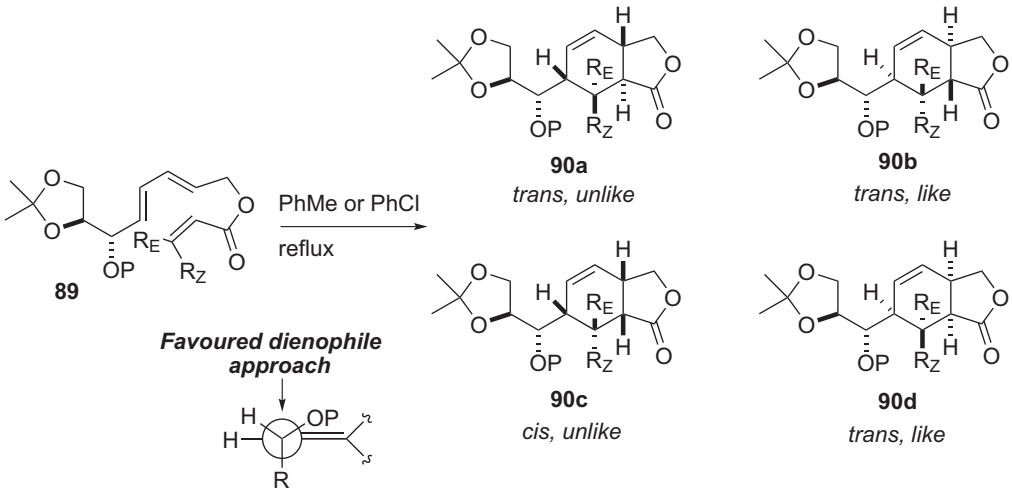

Scheme 40.

Table 9
Acyclic stereocontrol in the IMDA reaction

Entry	P	R_E	R_Z	*t* (h)	% Yield	Ratio **90 a/b/c/d**
1	H	H	CO_2Me	5	86	56:32:8:4
2	TMS	H	CO_2Me	12	67	80:14:4:2
3	TBS	H	CO_2Me	15	80	86:9:4:1
4	TIPS	H	CO_2Me	18	68	92:7:1:0
5	PNB	H	CO_2Me	12	95	49:39:6:6
6	TBS	CO_2Me	H	53	62	12:3:82:3

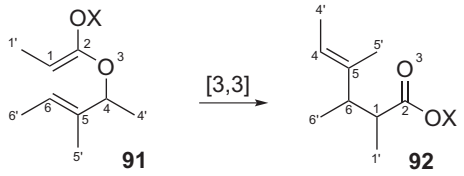

Scheme 41.

Yamazaki[75] and Martin[76] have shown examples of C1 exopericyclic stereocontrol using trifluoromethyl (**93**→**94**) and CO_2Bn (**97**→**98**) substituents, respectively (Scheme 42). In both cases, the observed stereoselectivity is rationalised by invoking the Cieplak model in which attack occurs antiperiplanar to the more electron-rich C–C σ bond. This allows for hyperconjugation between the C–R (or C–cyclopentyl) groups and the electron-deficient σ* orbital of the incipient C1–C6 bond. In the Yamazaki example, isosteric *i*-Pr and CF_3 substituents on **93** were used to remove steric bias from the transition-state model. Replacement of the CF_3 group by methyl (**95**→**96**) gave a significantly reduced selectivity.[77] Although deriving from different effects, this corresponds to reaction in the same sense, as predicted by the Felkin–Anh model.[78] Similar examples that occur in a Cieplak sense have been reported by Knight.[79] Other examples have been described of Johnson–Claisen rearrangements with chiral *ortho*lactones, although the selectivity in these processes is controlled by the relative energies of the chair and boat transition states.[80]

Attack in the opposite (non-Cieplak, anti-Felkin) sense has been reported by Fujisawa (**99**→**101**)[81] and Fleming (**102**→**103**) (Scheme 43) vide infra.[94] In these examples,[82] attack occurs preferentially anti to the most electronegative group, with the smallest substituent eclipsing the vinylic double bond to minimise 1,3-allylic strain, a reactive conformation, that is, commonplace in examples of C6 exopericyclic stereocontrol.

In addition to rearrangements with carbon stereocentres, examples have been reported using chiral C1-sulfur substituents. The first reactions of this type were reported by Metzner, in which thioketene acetals **104** underwent a thio-Claisen rearrangement to give thioesters **105** in very high diastereoselectivity (Scheme 44).[83] The transition states proposed to account for the sense of the selectivity were derived from the original Felkin model in which the best donor (in this case the sulfur lone pair) is placed antiperiplanar to the incipient bond. The oxygen is the smallest substituent and eclipses the ketene acetal (cf. hydrogen eclipsing in the above examples). Both *E*- and *Z*-transition states lead to the same product. Similar examples have been reported from our own laboratories in which C1-sulfoximine stereocentres are used for exopericyclic stereocontrol.[84] Recently, we have used this methodology for the stereoselective formation of cyclopropanes via a decarboxylative Claisen rearrangement (dCr).[85]

The earliest examples of exopericyclic stereocontrol adjacent to C6 used C6′ dioxolane substituents. *syn*-Selective Ireland–Claisen rearrangements of **106** to give **107a–d** were reported by Cha,[86] with variations in allylic *E*/*Z* geometry and C1 substituent (Scheme 45, Table 10). The transition states proposed to account for the selectivity follow a similar pattern to those described for rearrangements with C1 stereocentres.[87] In this case, the vinylic portion of the ketene acetal attacks antiperiplanar to the dioxolane C6′–O bond in the conformation where the C6′–H bond eclipses the allylic moiety. Similar, although significantly less selective, Johnson–Claisen rearrangements featuring C6′ dioxolane substituents have also been reported by Suzuki[88] and Takano.[89]

Notable in this case is the slight increase in selectivity upon changing the allylic geometry from *E* to *Z*, which is consistent with an allylic strain model, and the significantly reduced selectivity in the absence of a C1 substituent. Similar rearrangements have been

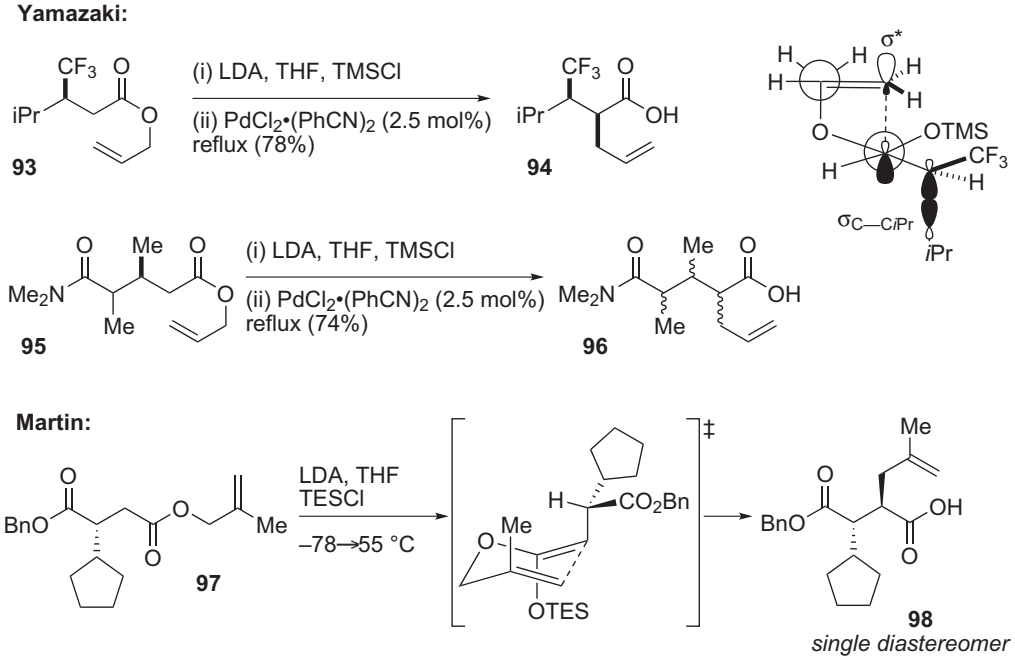

Scheme 42.

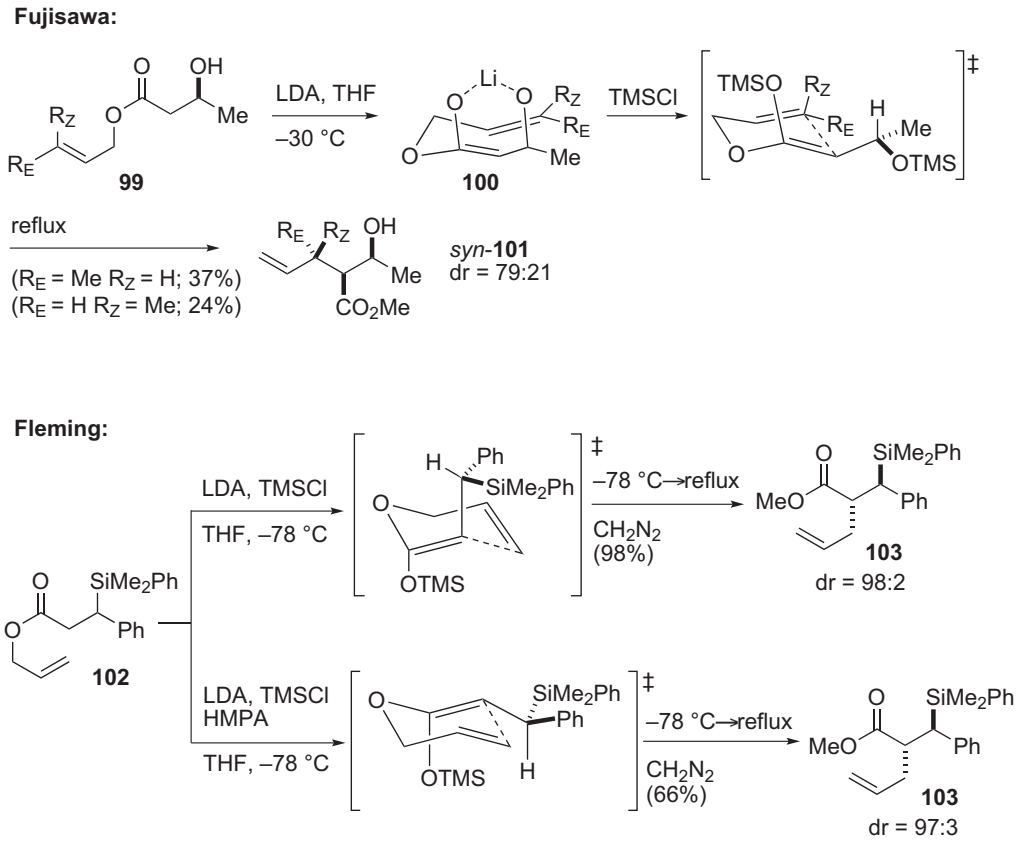

Scheme 43.

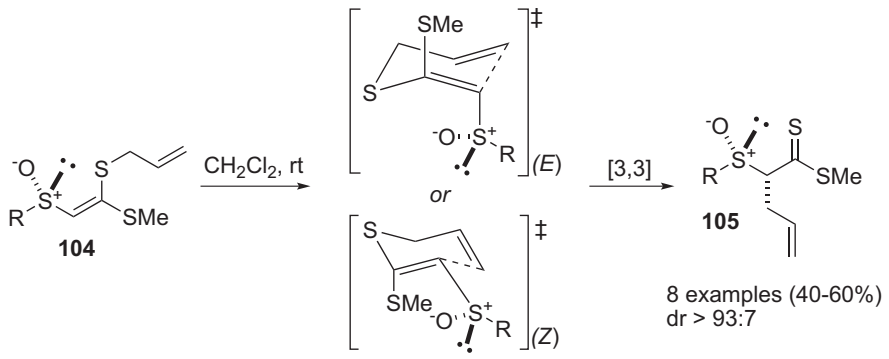

Scheme 44.

rationalised in terms of Houk's inside-alkoxy rule, although the sense of selectivity is the same.[57,90]

Highly diastereoselective rearrangements, in the same sense as those described by Cha and others (see above), have been reported with C6′ nitrogen substituents. Hauske[91] and Mulzer[92] studied the Ireland–Claisen rearrangements of the Boc-protected valine- and proline-derived substrates **108** and **110** to give **109** and **111**, respectively (Scheme 46).

Two complementary explanations for the high stereoselectivity were provided by Mulzer. The proposed transition state features, in common with other examples, antiperiplanar alignment of the C6′–N and the incipient C1–C6 bond, with the proline residue positioned in such a way that minimises 1,3-allylic strain. An additional explanation is given according to the model of Kahn and Hehre[68] (modified for the Claisen rearrangement) in which the most electrophilic face of the allylic moiety approaches the most nucleophilic face of the vinylic moiety.[93] The energy of the allylic LUMO is lowered via mixing of $\sigma^*_{C6'-N}$ and $\pi^*_{C=C}$ orbitals, while the vinylic π orbital (HOMO) is raised in energy by the two electron-donating OTMS and OBn residues. Overall, this leads to a strong HOMO–LUMO interaction, lowering the activation barrier of the rearrangement.

Fleming, in the same report that presented the effects of C1′ silicon stereocentres, also investigated the effects of C6′ silicon stereocentres in the rearrangement of **112** to **113** (Scheme 47).[94] Attack of the vinylic moiety antiperiplanar to the silicon substituent is maintained in all cases. Evidence for 1,3-allylic strain as a control element was shown by the high selectivity of *Z* substrates. The isomeric *E* substrates underwent rearrangement with moderate selectivity for the opposite diastereomer, which arises from a reactive conformation in which the methyl group is 'inside'. Calculations showed this conformation to be more populated than

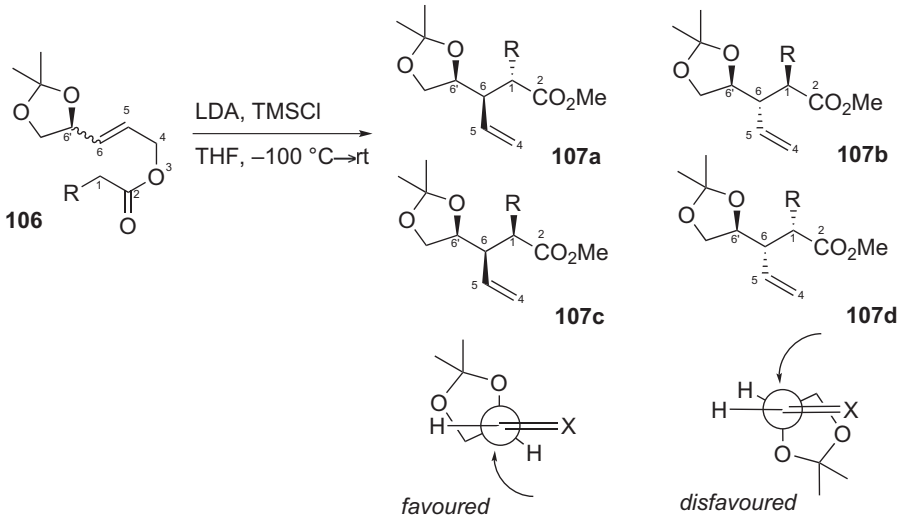

Scheme 45.

Table 10
Syn-Selective Ireland–Claisen rearrangements of **106**

Entry	*E*/*Z*	R	% Yield	Ratio **107a**/**b**/**c**/**d**
1	*E*	H	54	1:1.3
2	*E*	OMe	59	4.4:1:0.2:0.3
3	*E*	OCH_2OMe	50	4.0:1:0.3:0.2
4	*E*	OBn	48	4.2:1:0.3:0.1
5	*Z*	H	50	1:1.4
6	*Z*	OMe	48	0.5:0.3:9:1
7	*Z*	OCH_2OMe	51	0.1:0.2:1:0.2
8	*Z*	OBn	56	0.3:0.3:5:1

Work from our own laboratory has shown the importance of the allylic substitution pattern in determining stereoselectivity when C6′ stereocentres are present on the pericyclic array.[101] While *Z*-configured allylic alcohols bearing sulfide substituents *Z*-**122** rearrange with good selectivity for *syn*-**123**, the analogous *E*-configured allylic alcohols rearrange unselectively (Scheme 49, Table 11).

The differing behaviour can be rationalised by comparing four diastereomeric transition states, each of which possesses an antiperiplanar alignment of the C6′–heteroatom and incipient C1–C6 bond in common with the above examples (Scheme 50). For *Z*-**122**, the major product arises from an orientation where

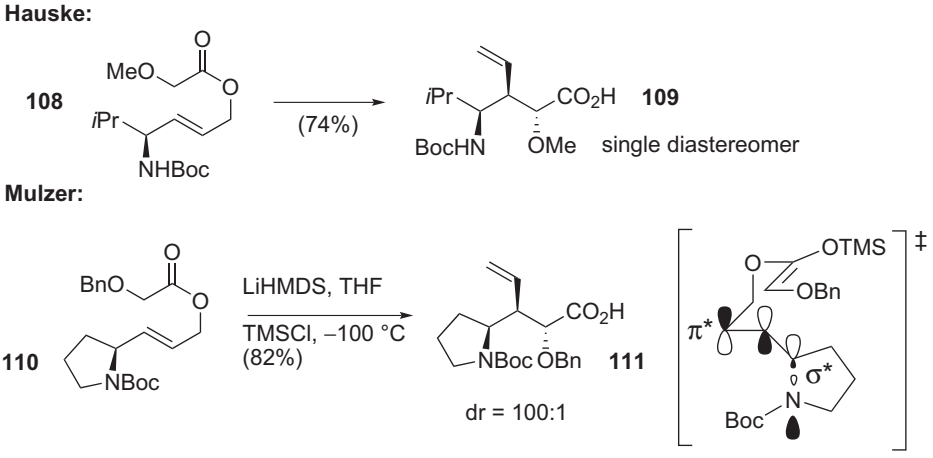

Scheme 46.

the alternative in which the hydrogen is 'inside'. This conformation is accessible in the absence of significant 1,3-allylic strain effects.[95]

Thio-Claisen rearrangements have also been used to study the effects of C6′ stereocentres.[96] In particular, numerous examples of exopericyclic stereocontrol from C6′ substituents in Belluš–Claisen[97] (ketene Claisen) rearrangements of allylic sulfides have been reported (**116**→**117** and **118**→**119**), which follow the established patterns.[98] The aza-analogues of these reactions have also been investigated (**120**→**121**) and reduced selectivity was reported for rearrangements lacking a C1 substituent on the pericyclic array (Scheme 48).[99] An additional example of a thio-Claisen rearrangement in the same sense was reported by Porter.[100]

the C6′–H bond eclipses the allylic C4–C5 bond (transition state **A**), rather than the C6′–R bond (transition state **B**). The lesser steric bulk associated with C5–H, compared to C4–C5, results in a lower selectivity for the *E*-configured substrates (transition states **C** and **D**).

In addition to the Claisen rearrangement, acyclic stereocontrol has also been reported in the related Overman rearrangement.[102] Chida reports an example of such a reaction during the synthesis of (+)-lactacystin.[103] Trichloracetimidate **124** underwent rearrangement upon heating in toluene to give **125** with good diastereoselectivity. The product is derived from a transition state that shares many common features with those of the Claisen

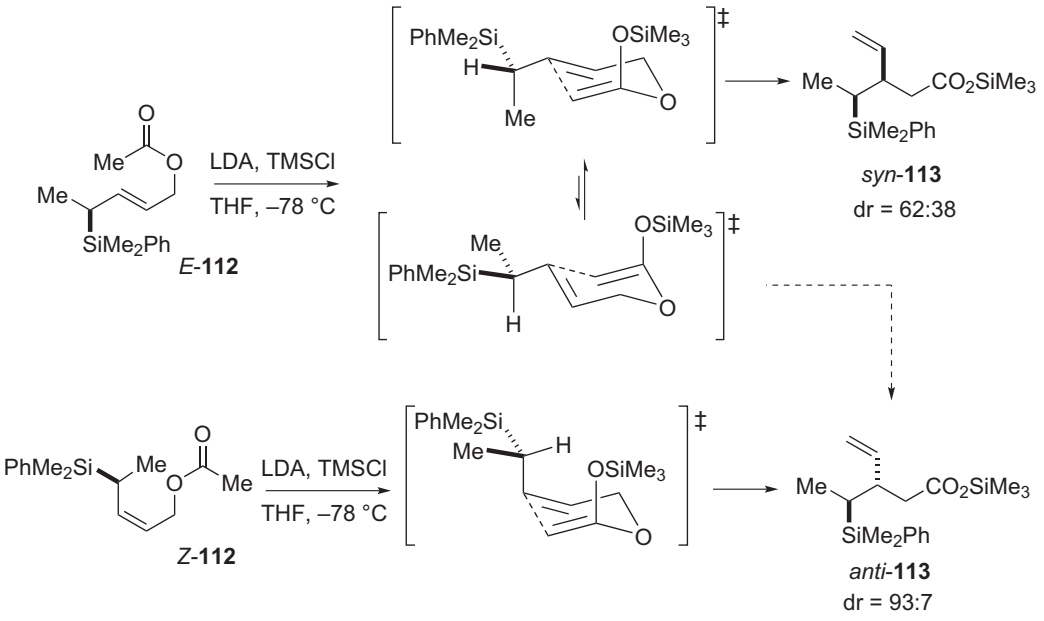

Scheme 47.

Ketene Claisen rearrangement:

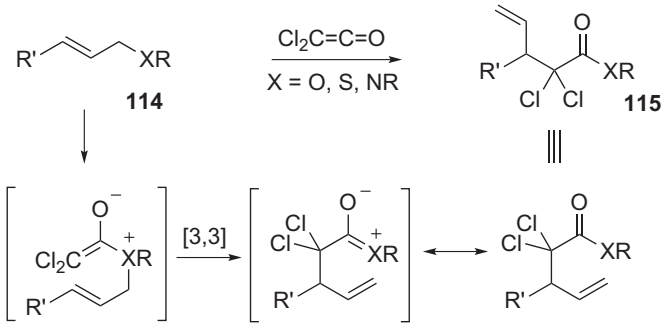

Allylic thioethers:

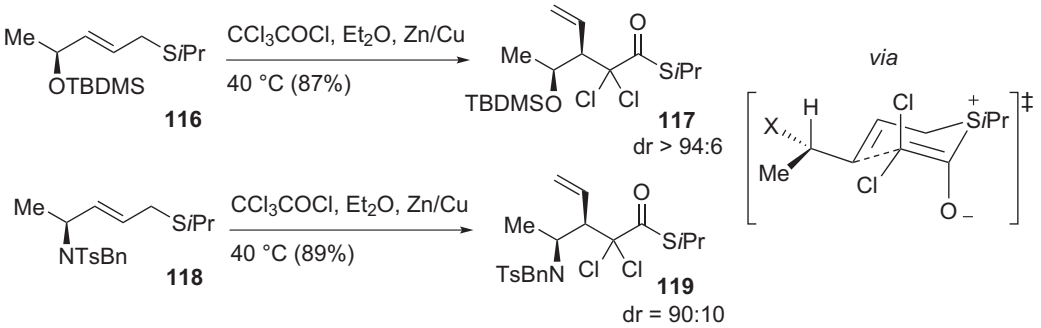

Allylic amines:

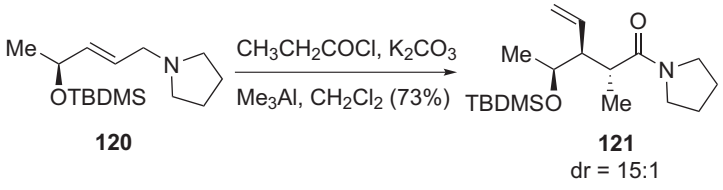

Scheme 48.

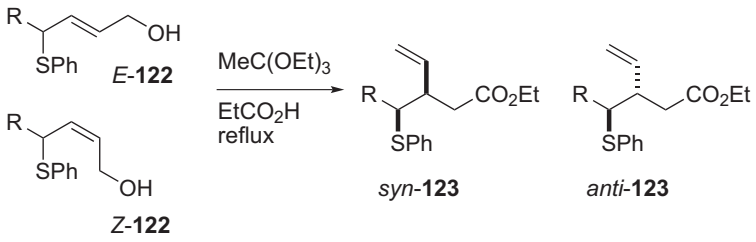

Scheme 49.

Table 11
Stereoselective Claisen rearrangements of allylic sulfides **122**

Entry	R	*E*/*Z*	Time (h)	% Yield	Ratio *syn*/*anti* **123**
1	Me	*E*	7	98	1:1
2	Me	*Z*	24	97	3:1
3	*n*-C_5H_{11}	*E*	12	98	1:1
4	*n*-C_5H_{11}	*Z*	48	94	5:1
5	*i*-Pr	*E*	24	93	3:2
6	*i*-Pr	*Z*	48	87	3:1

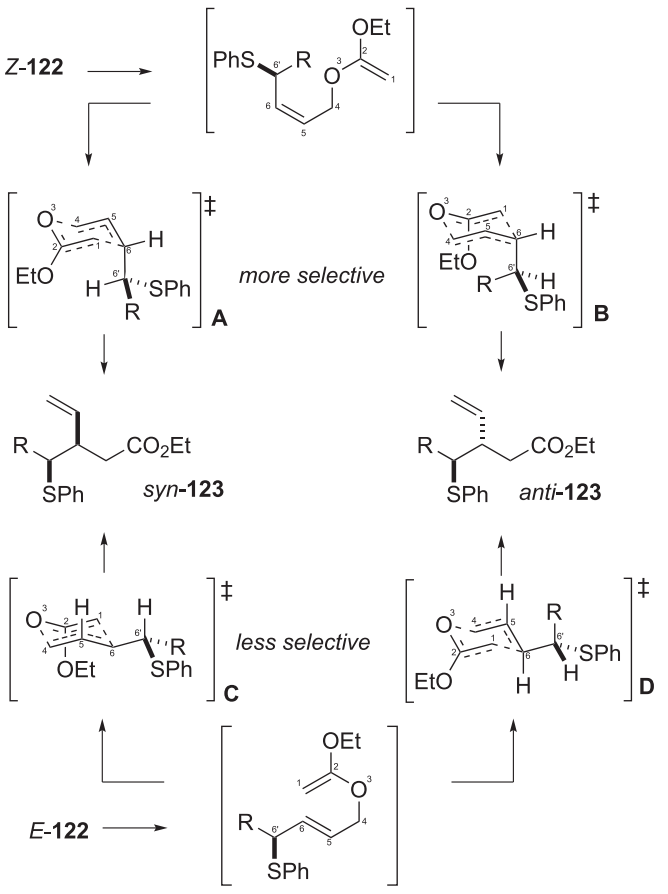

Scheme 50.

rearrangement, in particular the antiperiplanar alignment of the incipient C–N and furanose C–O bonds (Scheme 51).

4.4. [2,3]-Sigmatropic rearrangements

Examples of acyclic stereocontrol in [2,3]-sigmatropic rearrangements are comparatively scarce, compared to the related [3,3]-sigmatropic case. The seminal contribution to this area was made in 1988 by Brückner, who studied the [2,3]-Wittig rearrangement of allylic dioxolanes **126** and **128** to give **127** and **129**, respectively.[104] The rearrangement occurred in the *syn* sense, in the same fashion as the analogous Claisen rearrangements of allylic dioxolanes. In the transition state leading to the major *syn* product, the dioxolane C–O bond lies perpendicular to the allylic C=C bond, maintaining a favourable $\sigma^*_{C-O}/\pi^*_{C=C}$ overlap, which contributes to overall lowering of the LUMO. As shown by the complete *syn* selectivity in the rearrangement of *Z*-allylic substrate **128**, 1,3-allylic strain is a component of this model (Scheme 52).

Other examples have been reported of acyclic stereocontrol in similar [2,3]-Wittig rearrangements, and the above model explains these well.[105] More recently, Davies has reported stereoselective [2,3]-sigmatropic rearrangements of lithium *N*-benzyl-*O*-allylhydroxylamides.[106] The substrates studied possessed both all-hydrocarbon stereocentres **130** and heteroatom-bearing stereocentres **132**/**134**. In the latter case, both *E*- and *Z*-configured substrates were compared. All substrates underwent rearrangement to give the *syn* products **131**, **133** and **135**, respectively. For the all-hydrocarbon stereocentres, this can be explained using the same transition-state model as that of Brückner, with attack of the anion antiperiplanar to the phenyl group. For heteroatom-bearing stereocentres, this model predicts the opposite *anti* product, and a chelation transition state was proposed to explain the formation of the *syn* product (Scheme 53).

4.5. Conclusions

The models presented for describing acyclic stereocontrol in pericyclic reactions have seen less recent development, compared to those for acyclic stereocontrol in additions to carbonyls and double bonds. However, for both [3+2] and [4+2] cycloadditions the patterns of stereoselectivity are well defined. The inside-alkoxy model developed by Houk is widely applied. The model holds well for other heteroatomic groups, particularly fluorides. Exceptions to the rule occur when chelation or hydrogen-bonding interactions are possible

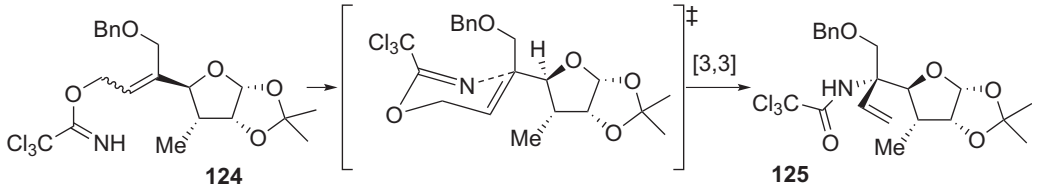

Scheme 51.

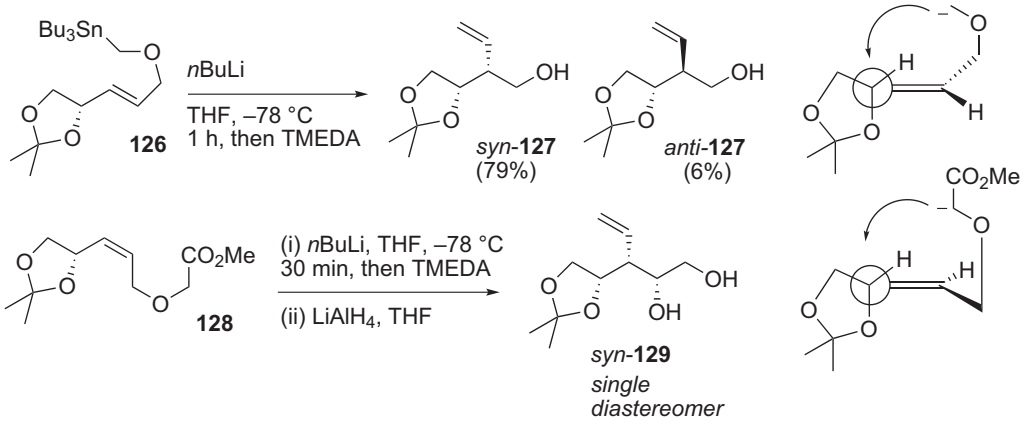

Scheme 52.

All-hydrocarbon stereocentres

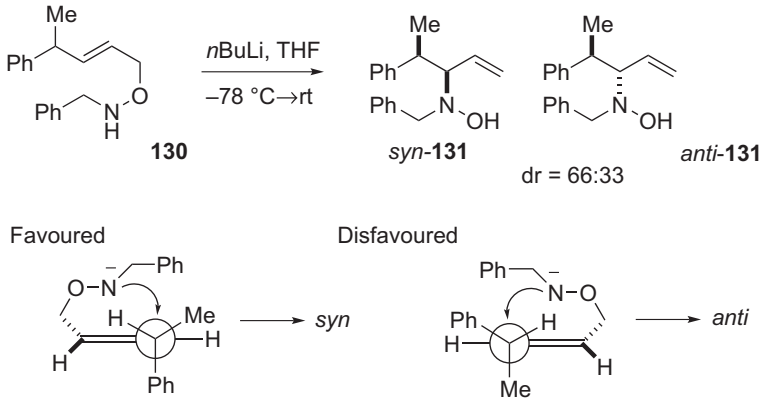

Heteroatom-bearing stereocentres

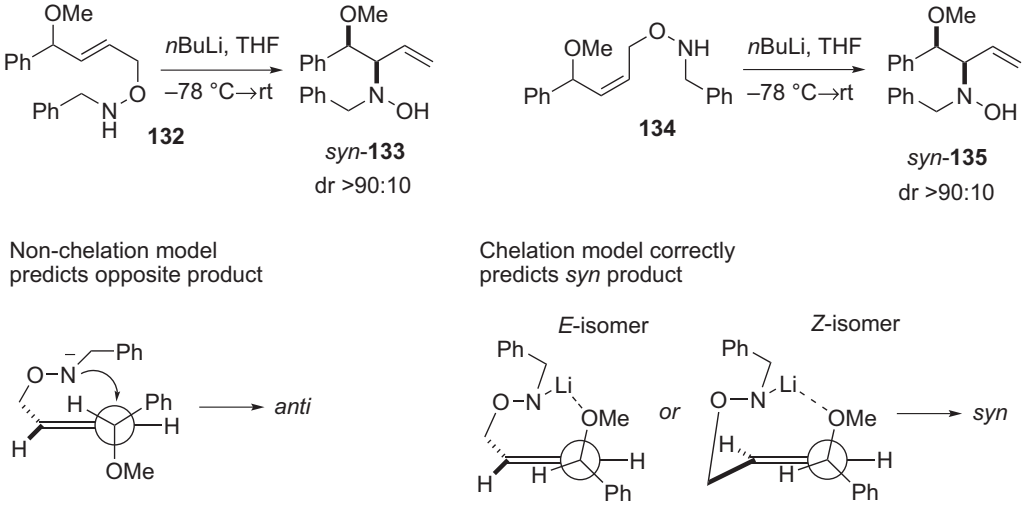

Scheme 53.

between the heteroatom on the stereocentre and the approaching reactant. Although models have been proposed that explain [3,3]- and [2,3]-sigmatropic rearrangements, there are comparatively few examples in the literature. In common with the reactions of C=C double bonds adjacent to a stereocentre, 1,3-allylic strain is an important factor in influencing acyclic stereocontrol.

5. Reactions adjacent to metal stereocentres

In addition to reactions of functional groups adjacent to carbon or sulfur stereocentres, acyclic stereocontrol is also possible for reactions of prochiral organic ligands on organometallic complexes. Widely explored in this sense are tricarbonyliron

complexes. The subject has been comprehensively reviewed by Cox and Ley.[107] A diene tricarbonyliron complex exhibits planar chirality. If the diene ligand contains an adjacent functional group, for example, in **136**, a carbonyl group, this may adopt a preferred reactive conformation with its two diastereotopic faces sterically differentiated by the tricarbonyliron moiety.[108] The s-*cis* and s-*trans* conformations of **137** are possible, but the latter is disfavoured by 1,3-allylic strain. Attack of approaching nucleophiles occurs *anti* to the bulky tricarbonyliron moiety. Aldehydes react with lower diastereoselectivity, due to the diminished interaction of the diene with the aldehydic hydrogen reducing the level of 1,3-allylic strain in the s-*trans* conformation (Scheme 54). Similar methodology has recently been used for the synthesis of 2-dienyl piperidines[109] and for controlling the sense of intramolecular pinacol couplings.[110] Other stereogenic iron complexes have been used to attain acyclic stereocontrol: substituted diphosphaferrocenes have recently been reported to control the sense of addition of phosphorus[111] and organometallic[112] nucleophiles to an adjacent aldehyde.

6. Summary

Recent developments in models for acyclic stereocontrol have been discussed in the context of three important classes of organic reaction and some recent organometallic reactions. For additions of nucleophiles to carbonyls with an adjacent stereocentre, both computational and experimental evidence have challenged the predominance of the Felkin–Anh and Cram models for predicting stereoselectivity. Various models for describing electrophilic and nucleophilic addition to double bonds have been proposed that account for variations in selectivity. However, these are often very specific to each particular reaction. In some cases, the major product arises from a seemingly high-energy transition state, e.g., in examples of the inside-methyl effect. Above all, 1,3-allylic strain appears to be the most important control element in reactions of C=C double bonds adjacent to a stereocentre. Many of the same models have been extended to explain acyclic stereocontrol in pericyclic reactions. In these cases, both stereoelectronic effects, again 1,3-allylic strain in particular, and electrostatic effects must be taken into account. Stereoselective reactions of unsaturated functional groups adjacent to organometallic complexes are also emerging as useful tools for establishing acyclic stereocontrol.

Taking into account the above examples, some general conclusions can be drawn. There is no unified theory that explains all modes of acyclic stereocontrol. Rather, it appears that models are very specific to the individual reaction mechanism, and the nature of the incoming electrophile or nucleophile must be considered.

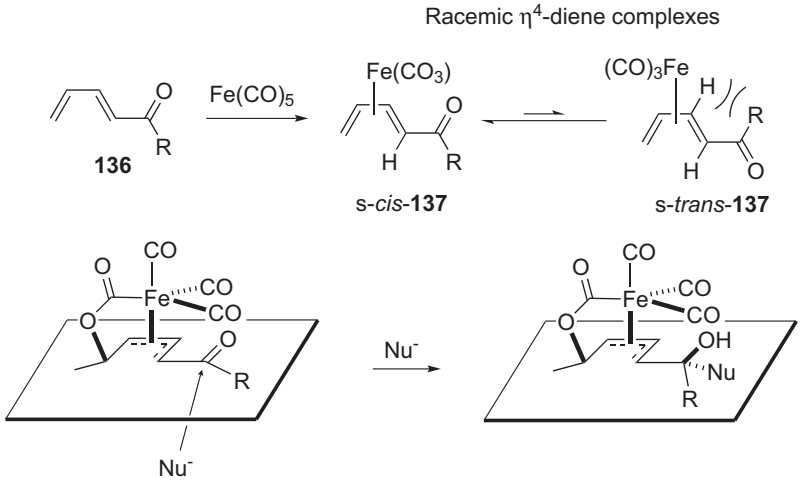

Scheme 54.

This chemistry is not limited to iron complexes; tungsten-*syn*-π-pentadienyl complexes have been used to effect acyclic stereocontrol in the preparation of adjacent 1,3-diols. The Lewis-acid-promoted Prins reaction of the tungsten complex **139**, derived from **138**, with an aldehyde affords a η^4-*trans*-diene cationic intermediate **140**, which undergoes hydrolysis with water *anti* to the bulky complex to give **141** (Scheme 55).[113] This class of reaction is emerging as an interesting new area for investigations into acyclic stereocontrol.

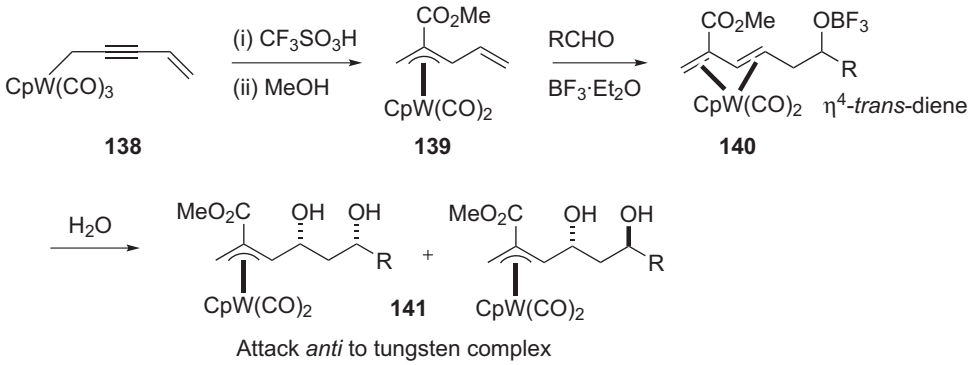

Scheme 55.

Additional complexity is encountered when stereoselectivity is a function of both acyclic and cyclic stereocontrol (double diastereoselection). These cannot be considered in isolation and models must take into account interactions between cyclic and acyclic transition states. Developments in computational methods have contributed to our ability to predict the sense of acyclic stereocontrol, although exceptions to these predictions are often encountered in experiments. Development of models and methods for establishing acyclic stereocontrol remains a highly active area of interest in synthetic chemistry.

Acknowledgements

The author wishes to thank Professor Donald Craig for his continued support. EPSRC and Pfizer are thanked for funding (supported DTA studentship to A.G.O.).

References and notes

1. Fischer, E. *Ber. Dtsch. Chem. Ges.* **1894**, *27*, 3189–3232.
2. Zimmerman, H. E.; Traxler, M. D. *J. Am. Chem. Soc.* **1957**, *79*, 1920–1923.
3. *The Claisen Rearrangement*; Hiersemann, M., Nubbemeyer, U., Eds.; Wiley: Weinheim, 2007.
4. (a) Heathcock, C. H. *Science* **1981**, *214*, 395–400; (b) Bartlett, P. A. *Tetrahedron* **1980**, *36*, 1–72; (c) Mahrwald, R. *Chem. Rev.* **1999**, *99*, 1095–1120; (d) Mengel, A.; Reiser, O. *Chem. Rev.* **1999**, *99*, 1191–1223.
5. Cram, D. J.; Elhafez, F. A. A. *J. Am. Chem. Soc.* **1952**, *74*, 5828–5835.
6. Cornforth, J. W.; Cornforth, MR. H.; Matthew, K. *J. Chem. Soc.* **1959**, 112–127.
7. (a) Karabatsos, G. J. *Tetrahedron Lett.* **1972**, *13*, 5289–5292; (b) Karabatsos, G. J.; Althuis, T. H. *Tetrahedron Lett.* **1967**, *8*, 4911–4914; (c) Karabatsos, G. J. *J. Am. Chem. Soc.* **1967**, *89*, 1367–1371.
8. Chérest, M.; Felkin, H.; Prudent, N. *Tetrahedron Lett.* **1968**, *9*, 2199–2204.
9. (a) Anh, N. T. *Top. Curr. Chem.* **1980**, *88*, 145–162; (b) Anh, N. T.; Eisenstein, O. *Nouv. J. Chim.* **1977**, *1*, 61–70; (c) Anh, N. T.; Eisenstein, O. *Tetrahedron Lett.* **1976**, *17*, 155–158; (d) Eisenstein, O.; Hoffmann, R. *J. Am. Chem. Soc.* **1980**, *102*, 6148–6149; (e) Anh, N. T.; Eisenstein, O.; Lefour, J.-M.; Dâu, M.-E. *J. Am. Chem. Soc.* **1973**, *95*, 6146–6147.
10. (a) Bürgi, H. B.; Dunitz, J. D.; Shefter, E. *J. Am. Chem. Soc.* **1973**, *95*, 5065–5067; (b) Bürgi, H. B.; Dunitz, J. D.; Lehn, J. M.; Wipff, G. *Tetrahedron* **1974**, *30*, 1561–1572.
11. Roush, W. R. *J. Org. Chem.* **1991**, *56*, 4151–4157 and references therein.
12. Gennari, C.; Vieth, S.; Comotti, A.; Vulpetti, A.; Goodman, J. M. *Tetrahedron* **1992**, *48*, 4439–4458.
13. (a) Roush, W. R.; Adam, M. A.; Walts, A. E.; Harris, D. J. *J. Am. Chem. Soc.* **1986**, *108*, 3422–3434; (b) Brinkmann, H.; Hoffmann, R. W. *Chem. Ber.* **1990**, *123*, 2395–2401.
14. The Cornforth model has also been modified to incorporate the Bürgi–Dunitz trajectory and torsional effects: see Ref. 28.
15. Gung, B. W.; Xue, X. *Tetrahedron: Asymmetry* **2001**, *12*, 2955–2959.
16. Batey, R. A.; Thadani, A. N. *Tetrahedron Lett.* **2003**, *44*, 8051–8055.
17. Evans, D. A.; Siska, S. J.; Cee, V. J. *Angew. Chem., Int. Ed.* **2003**, *42*, 1761–1765.
18. Cee, V. J.; Cramer, C. J.; Evans, D. A. *J. Am. Chem. Soc.* **2006**, *128*, 2920–2930.
19. For theoretical studies in support of the Cornforth model, see: (a) Cieplak, A. S.; Wiberg, K. B. *J. Am. Chem. Soc.* **1992**, *114*, 9226–9227; (b) Frenking, G.; Köhler, K. F.; Reetz, M. T. *Tetrahedron* **1994**, *50*, 11197–11204; another treatment of these models using visualisation of orbitals, see: Wilmot, N.; Marsella, M. J. *Org. Lett.* **2006**, *8*, 3109–3112.
20. (a) Evans, D. A.; Welch, D. S.; Speed, A. W. H.; Moniz, G. A.; Reichelt, A.; Ho, S. *J. Am. Chem. Soc.* **2009**, *131*, 3840–3841; (b) Floreancig, P. E. *Angew. Chem., Int. Ed.* **2009**, *48*, 7736–7739.
21. For further examples of double diastereoselection in aldol reactions rationalised using Cornforth-type transition states see: (a) Días-Oltra, S.; Murga, J.; Falomir, E.; Carda, M.; Peris, G.; Marco, J. A. *J. Org. Chem.* **2005**, *70*, 8130–8139; (b) Marco, J. A.; Carda, M.; Días-Oltra, S.; Murga, J.; Falomir, E.; Roeper, H. *J. Org. Chem.* **2003**, *68*, 8577–8582 and references therein; (c) Zhang, Y.; Sammakia, T. *J. Org. Chem.* **2006**, *71*, 6262–6265.
22. Días-Oltra, S.; Carda, M.; Murga, J.; Falomir, E.; Marco, J. A. *Chem.—Eur. J.* **2008**, *14*, 9240–9254.
23. Smith, R. J.; Trzoss, M.; Bühl, M.; Bienz, S. *Eur. J. Org. Chem.* **2002**, 2770–2775.
24. Houk, K. N. *Theor. Chem. Acc.* **2000**, *103*, 330–331.
25. For a study showing reactant conformation to be more important than hyperconjugative effects in carbene insertion reactions, see: Kaneno, D.; Tomoda, S. *Org. Lett.* **2003**, *5*, 2947–2949.
26. For recent examples see: (a) Jeon, S.-J.; Fisher, E. J.; Carroll, P. J.; Walsh, P. J. *J. Am. Chem. Soc.* **2006**, *128*, 9618–9619; (b) Nebot, J.; Figueras, S.; Romea, P.; Urpí, F.; Ji, Y. *Tetrahedron* **2006**, *62*, 11090–11099; (c) McNulty, J.; Nair, J. J.; Sliwinski, M.; Harrington, L. E.; Pandey, S. *Eur. J. Org. Chem.* **2007**, 5669–5673; (d) Kang, B.; Britton, R. *Org. Lett.* **2007**, *9*, 5083–5086; (e) Burton, J. W.; Anderson, E. A.; O'Sullivan, P. T.; Collins, I.; Davies, J. E.; Bond, A. D.; Feeder, N.; Holmes, A. B. *Org. Biomol. Chem.* **2008**, *73*, 2240–2255; (f) Ruiz, M.; Ruanova, T. M.; Blanco, O.; Núñez, F.; Pato, C.; Ojea, V. *J. Org. Chem.* **2008**, *73*, 2240–2255; (g) Kang, B.; Mowat, J.; Pinter, T.; Britton, R. *Org. Lett.* **2009**, *11*, 1717–1720.
27. For early studies, see: (a) Chautemps, P.; Pierre, J.-L. *Tetrahedron* **1976**, *32*, 549–557; (b) Chamberlain, P.; Roberts, M. L.; Witham, G. *J. Chem. Soc. B* **1970**, 1374–1381.
28. Paddon-Row, M. N.; Rondan, N. G.; Houk, K. N. *J. Am. Chem. Soc.* **1982**, *104*, 7162–7166.
29. Paddon-Row, M. N.; Rondan, N. G.; Wu, Y.-D.; Metz, J. T.; Houk, K. N. *Tetrahedron* **1984**, *40*, 2257–2274.
30. Kishi, Y. *Aldrichimica Acta* **1980**, *13*, 23–30.
31. Cha, J. K.; Christ, W. J.; Kishi, Y. *Tetrahedron* **1984**, *40*, 2247–2255.
32. Hoffmann, R. W. *Chem. Rev.* **1989**, *89*, 1841–1860.
33. Donohoe, T. J.; Johnson, P. D.; Pye, R. J.; Keenan, M. *Org. Lett.* **2004**, *6*, 2583–2585.
34. Treament of an analogous allylic methyl ether with OsO_4–TMEDA gave a 50: 50 mixture of *syn* and *anti* diastereomers.
35. For a similar example of aminohydroxylation, see: Ref. 33.
36. Fleming, I. Stereocontrol in Organic Synthesis Using Silicon Compounds In *Frontiers in Natural Product Chemistry*; Attur-ur-Rahman, Choudary, I., Kahn, K. M., Eds.; 2005; pp 55–64 Bentham: Bentham Scientific Publishers. http://dx.doi.org/10.2174/1574089054583731.
37. For a recent review on polypropionate synthesis, see: Jun, L.; Menche, D. *Synthesis* **2009**, 2293–2315.
38. (a) Kireev, A. S.; Manpadi, M.; Kornienko, A. *J. Org. Chem.* **2006**, *71*, 2630–2640; (b) Manpadi, M.; Kornienko, A. *Tetrahedron* **2005**, *46*, 4433–4437.
39. For recent examples, see: (a) Hanessian, S.; Reddy, G. J.; Chahal, N. *Org. Lett.* **2006**, *8*, 5477–5840; (b) Hanessian, S.; Chahal, N.; Giroux, S. *J. Org. Chem.* **2006**, *71*, 5694–5707; (c) Carreño, M. C.; Sanz-Cuesta, M. J. *J. Org. Chem.* **2005**, *70*, 10036–10045; (d) Hanessian, S.; Mascitti, V.; Giroux, S. *Proc. Acad. Natl. Sci. U.S.A.* **2004**, *101*, 11996–12001; (e) Hanessian, S.; Ma, J.; Wang, W. *J. Am. Chem. Soc.* **2001**, *123*, 10200–10206.
40. (a) Roush, W. R.; Lesur, B. M. *Tetrahedron Lett.* **1983**, *24*, 2231–2234; (b) Roush, W. R.; Michaelides, M. R.; Tai, D. F.; Lesur, B. M.; Chong, W. K. M.; Harris, D. J. *J. Am. Chem. Soc.* **1989**, *111*, 2984–2995.
41. (a) Yamamoto, Y.; Nishii, S.; Ibuka, T. *J. Chem. Soc., Chem. Commun.* **1987**, 464–466; (b) Yamamoto, Y.; Chounan, Y.; Nishii, S.; Ibuka, T.; Kitahara, H. *J. Am. Chem. Soc.* **1992**, *114*, 7652–7660.
42. For a review, see: Cieplak, A. S. *Chem. Rev.* **1999**, *99*, 1265–1336.
43. For brevity, only the results of diphenylcuprate addition are shown. Addition of other diarylcuprates followed the same pattern.
44. Nakamura, E.; Mori, S. *Angew. Chem., Int. Ed.* **2000**, *39*, 3750–3771.
45. For similar examples, see Ref. 21 within Ref. 38a (this document).
46. Hanessian, S.; Sumi, K. *Synthesis* **1991**, 1083–1089 and references therein.
47. Garner, P.; Ramakanth, S. *J. Org. Chem.* **1986**, *51*, 2609–2612.
48. Rastogi, S. K.; Kornienko, A. *Tetrahedron: Asymmetry* **2006**, *17*, 3170–3178.
49. Betson, M. S.; Fleming, I.; Ouzman, J. V. A. *Org. Biomol. Chem.* **2003**, *1*, 4017–4024.
50. (a) Spangenberg, T.; Schoenfelder, A.; Breit, B.; Mann, A. *Org. Lett.* **2007**, *9*, 3881–3884 for previous examples of directed allylic substitution in this manner, see: (b) Breit, B.; Demel, P. *Adv. Synth. Catal.* **2001**, *343*, 429–432; (c) Demel, P.; Keller, M.; Breit, B. *Chem.—Eur. J.* **2006**, *12*, 6669–6683.
51. For recent discussions see: (a) Davies, S. G.; Durbin, M. J.; Goddard, E. C.; Kelly, P. M.; Kurosawa, W.; Lee, J. A.; Nicholson, R. L.; Price, P. D.; Roberts, P. M.; Russell, A. J.; Scott, P. M.; Smith, A. D. *Org. Biomol. Chem.* **2009**, *7*, 761–776; (b) Cailleau, T.; Cooke, J. W. B.; Davies, S. G.; Ling, K. B.; Naylor, A.; Nicholson, R. L.; Price, P. D.; Roberts, P. M.; Russell, A. J.; Smith, A. D.; Thomson, J. E. *Org. Biomol. Chem.* **2007**, *5*, 3922–3931.
52. For a related reaction, see: Barrett, A. G. M.; Weipert, P. D.; Dhanak, D.; Husa, R. K.; Lebold, S. A. *J. Am. Chem. Soc.* **1991**, *113*, 9820–9824.
53. Moglioni, A. G.; Muray, E.; Castillo, J. A.; Álvarez-Larena, Á; Moltrasio, G. Y.; Branchadell, V.; Otuño, J. *Org. Chem.* **2002**, *67*, 2402–2410.
54. Mulzer, J.; Kappert, M.; Huttner, G.; Jibril, I. *Angew. Chem., Int. Ed. Engl.* **1984**, *23*, 704–705.
55. Segura, A.; Csákÿ, A. G. *Org. Lett.* **2007**, *9*, 3667–3670.
56. Raimondi, L.; Benaglia, M. *Eur. J. Org. Chem.* **2001**, 1033–1043.
57. Houk, K. N.; Moses, S. R.; Wu, Y.-D.; Rondan, N. G.; Jäger, V.; Schohe, R.; Fronczek, F. R. *J. Am. Chem. Soc.* **1984**, *106*, 3880–3882.
58. (a) Annunziata, R.; Cinquini, M.; Cozzi, F.; Gennari, C.; Raimondi, L. *J. Org. Chem.* **1989**, *52*, 4674–4681; (b) Annunziata, R.; Cinquini, M.; Cozzi, F.; Dondio, G.; Raimondi, L. *Tetrahedron* **1987**, *43*, 2369–2380.
59. (a) Boyd, E. C.; Paton, M. P. *Tetrahedron Lett.* **1993**, *34*, 3169–3172 for a recent example, see; (b) Pinto, A.; Conti, P.; De Amici, M.; Tamborini, L.; Madsen, U.; Nielsen, B.; Cristesen, T.; Bräuner-Osborne, H.; De Micheli, C. *J. Med. Chem.* **2008**, *51*, 2311–2315.
60. (a) Conti, P.; De Amici, M.; Roda, G.; Pinto, A.; Tamborini, L.; Madsen, U.; Nielsen, B.; Bräuner-Osborne, H.; De Micheli, C. *Tetrahedron* **2007**, *63*, 2249–2256; (b) Schreiner, E. P.; Gstach, H. *Synlett* **1996**, 1131–1133.
61. Prakesch, M.; Grée, D.; Grée, R.; Carter, J.; Washington, I.; Houk, K. N. *Chem.—Eur. J.* **2003**, *9*, 5664–5672.
62. Additional evidence for an inside fluorine effect: Tredwell, M.; Luft, J. A. R.; Schuler, M.; Tenza, K.; Houk, K. N. *Angew. Chem., Int. Ed.* **2008**, *47*, 357–360.
63. (a) Lohse-Fraefel, N.; Carreira, E. M. *Org. Lett* **2005**, *7*, 2011–2014 for an additional example, see: (b) Kociolek, M. G.; Hongfa, C. *Tetrahedron Lett.* **2003**, *44*, 1811–1813.
64. Luft, J. A. R.; Meleson, K.; Houk, K. N. *Org. Lett.* **2007**, *9*, 555–558.
65. Shang, Y.; Feng, Z.; Yuan, L.; Wang, S. *Tetrahedron* **2008**, *64*, 5779–5783.

66. Padwa, A.; Prein, M. *Tetrahedron* **1998**, *54*, 6957–6976.
67. For a similar example of an amide stereocentre controlling a Claisen rearrangement, see: Davies, S. G.; Garner, A.; Nicholson, R. L.; Osborne, J.; Roberts, P. M.; Savory, E. D.; Smith, A. D.; Thomson, J. E. *Org. Biomol. Chem.* **2009**, *7*, 2604–2611.
68. Kahn, S. D.; Hehre, W. J. *J. Am. Chem. Soc.* **1987**, *109*, 663–666.
69. For a recent studies of stereoselectivity in the polar hetero-Diels–Alder reaction, see: (a) Sumway, W.; Ham, S.; Moer, J.; Whittlesey, B. R.; Birney, D. M. *J. Org. Chem.* **2000**, *65*, 7731–7739; (b) Alajarín, M.; Cabrera, J.; Pastor, A.; Sánchez-Andrada, P.; Bautista, D. *J. Org. Chem.* **2008**, *73*, 963–973.
70. Haller, J.; Niwayama, S.; Duh, H.-Y.; Houk, K. N. *J. Org. Chem.* **1997**, *62*, 5728–5731.
71. Grée, D.; Vallerie, L.; Grée, R.; Toupet, L.; Washington, I.; Pelicier, J.-P.; Villacampa, M.; Pérez, J. M.; Houk, K. N. *J. Org. Chem.* **2001**, *66*, 2374–2381.
72. (a) Lilly, M. J.; Miller, N. A.; Edwards, A. J.; Willis, A. C.; Turner, P.; Paddon-Row, M. N.; Sherburn, M. S. *Chem.—Eur. J.* **2005**, 2525–2536; (b) Tripoli, R.; Cayzer, T. N.; Willis, A. C.; Sherburn, M. S.; Paddon-Row, M. N. *Org. Biomol. Chem.* **2007**, *5*, 2606–2616.
73. Nubbemeyer, U. *Synthesis* **2003**, *7*, 961–1008.
74. For an example of C4′ stereocentres, see: (a) Heathcock, C. H.; Finkelstein, B. L.; Jarvi, E. T.; Radel, P. A.; Hadley, C. R. *J. Org. Chem.* **1988**, *53*, 1922–1942 for an example of C5′ stereocentres, see: (b) Ishizaki, M.; Niimi, Y.; Hoshino, O. *Chem. Lett.* **2001**, *30*, 546–547.
75. Yamazaki, T.; Shinohara, N.; Kitazume, T.; Sato, S. *J. Org. Chem.* **1995**, *60*, 8140–8141.
76. (a) Pratt, L. M.; Bowles, S. A.; Courtney, S. F.; Hidden, C.; Lewis, C. N.; Martin, F. M.; Todd, R. S. *Synlett* **1998**, 531–533; (b) Pratt, L. M.; Beckett, R. P.; Bellamy, C. L.; Corkill, D. J.; Cossins, J.; Courtney, P. F.; Davies, S. J.; Davidson, A. H.; Drummond, A. H.; Helfrich, K.; Lewis, C. N.; Mangan, M.; Martin, F. M.; Miller, K.; Nayee, P.; Ricketts, M. L.; Thomas, W.; Todd, R. S.; Whittaker, M. *Bioorg. Med. Chem. Lett.* **1998**, *8*, 1359–1364.
77. Bott, G.; Field, L. D.; Sternhell, S. *J. Am. Chem. Soc.* **1980**, *102*, 5618–5626.
78. For a comparison of the Felkin–Anh and Cieplak models in a closely related system, see: Yamazaki, T.; Ichige, T.; Takei, S.; Kawashita, S.; Kitazume, T.; Kubota, T. *Org. Lett.* **2001**, *3*, 2915–2918.
79. (a) Knight, D. W.; Share, A. C.; Gallagher, P. T. *J. Chem. Soc., Perkin Trans. 1* **1991**, 1615–1616; (b) Knight, D. W.; Share, A. C.; Gallagher, P. T. *J. Chem. Soc., Perkin Trans. 1* **1997**, 2089–2097.
80. (a) Takahashi, T.; Miyazawa, M.; Sakamoto, Y.; Yamada, H. *Synlett* **1994**, 902–904; (b) Ziegler, F. E.; Thottathil, J. K. *Tetrahedron Lett.* **1982**, *23*, 3531–3534.
81. Fujisawa, T.; Tajima, K.; Ito, M.; Sato, T. *Chem. Lett.* **1984**, 1169–1172.
82. The selectivity in these examples is also in the opposite sense to: Beslin, P.; Perrio, S. *Tetrahedron* **1991**, *47*, 6275–6286; another report, with an ambiguous sense of stereoselectivity see: Kurth, M. J.; Yu, C.-M. *Tetrahedron Lett.* **1984**, *25*, 5003–5006.
83. (a) Alayrac, C.; Fromont, C.; Metzner, P.; Anh, N. T. *Angew. Chem., Int. Ed.* **1997**, *36*, 371–374; (b) Nowaczyk, S.; Alayrac, C.; Reboul, V.; Metzner, P.; Averbuch-Pouchot, M.-T. *J. Org. Chem.* **2001**, *66*, 7841–7848; (c) Désert, S.; Metzner, P.; Ramdani, M. *Tetrahedron* **1992**, *48*, 10315–10326.
84. Craig, D.; Grellepois, F.; White, A. J. P. *J. Org. Chem.* **2005**, *70*, 6827–6832.
85. Craig, D.; Gore, S. J.; Lansdell, M. I.; Lewis, S. E.; Mayweg, A. V. W.; White, A. J. P. *Chem. Commun.* **2010**, 4991–4993.
86. Cha, J. K.; Lewis, S. C. *Tetrahedron Lett.* **1984**, *25*, 5263–5266.
87. For a conflicting example in which Cieplak effects are dominant, see: Yadav, V. K.; Jeyaraj, D. A.; Parvez, M.; Yamdagni, R. *J. Org. Chem.* **1999**, *64*, 2928–2932.
88. Suzuki, T.; Sato, E.; Kamada, S.; Tada, H.; Unno, K. *J. Chem. Soc., Perkin Trans. 1* **1986**, 387–391.
89. Takano, S.; Kurotaki, A.; Takahashi, M.; Ogasawara, M. J. *J. Chem. Soc., Perkin Trans. 1* **1987**, 91–97.
90. Takano, S.; Seijo, K.; Hatakeyama, S. *Tetrahedron Lett.* **1985**, *26*, 865–868.
91. Hauske, J. R.; Julin, S. M. *Tetrahedron Lett.* **1993**, *34*, 4909–4912.
92. Mulzer, J.; Shanyoor, M. *Tetrahedron Lett.* **1993**, *34*, 6545–6548.
93. Kahn, S. D.; Hehre, W. J. *J. Am. Chem. Soc.* **1987**, *109*, 650–663.
94. Fleming, I.; Betson, M. S. *Org. Biomol. Chem.* **2003**, *1*, 4005–4016.
95. Yamamoto, Y.; Nishii, S.; Ibuka, T. *J. Chem. Soc., Chem. Commun.* **1987**, 1572–1573.
96. For an early example, see: Désert, S.; Metzner, P. *Tetrahedron* **1992**, *48*, 10327–10338.
97. (a) Malherbe, R.; Belluš, D. *Helv. Chim. Acta* **1978**, *61*, 3096–3099; (b) Gonda, J. *Angew. Chem., Int. Ed.* **2004**, *43*, 3516–3524 for leading references on exo-pericyclic stereocontrol see: (c) Craig, D.; King, N. P.; Mountford, D. M. *Chem. Commun.* **2007**, 1077–1079.
98. (a) Gonda, J.; Martinková, M.; Ernst, B.; Belluš, D. *Tetrahedron* **2001**, *57*, 5607–5613; (b) Nubbemeyer, U.; Öhrlein, R.; Gonda, J.; Ernst, B.; Belluš, D. *Angew. Chem., Int. Ed. Engl.* **1991**, *30*, 1465–1467; (c) Nubbemeyer, U.; Jeschke, R.; Öhrlein, R.; Gonda, J.; Ernst, B.; Belluš, D. *Helv. Chim. Acta* **1997**, *80*, 876–891.
99. (a) Nubbemeyer, U. *J. Org. Chem.* **1995**, *60*, 3773–3780; (b) Nubbemeyer, U. *J. Org. Chem.* **1996**, *61*, 3677–3686; (c) Deur, C. J.; Miller, M. W.; Hegedus, L. S. *J. Org. Chem.* **1996**, *61*, 2871–2876.
100. Ellwood, A. R.; Mortimer, A. J. P.; Tocher, D. A.; Porter, M. J. *Synlett* **2008**, 2199–2203.
101. Craig, D.; Harvey, J. W.; O'Brien, A. G.; White, A. J. P. *Chem. Commun.* **2010**, 6932–6934.
102. For additional recent examples, see: (a) Swift, M. D.; Sutherland, A. *Tetrahedron Lett.* **2007**, *48*, 3771–3773; (b) Jaunzeme, I.; Jirgensons, A.; Kauss, V.; Liepins, E. *Tetrahedron Lett.* **2006**, *47*, 3885–3887; (c) Jamieson, A. G.; Sutherland, A. *Tetrahedron* **2007**, *63*, 2123–2131; (d) Jamieson, A. G.; Sutherland, A. *Org. Biomol. Chem.* **2006**, *4*, 2932–2937.
103. (a) Chida, N.; Takeoka, J.; Tsutsumi, N.; Ogawa, S. *J. Chem. Soc., Chem. Commun.* **1995**, 793–794; (b) Masse, C. E.; Morgan, A. J.; Adams, J.; Panek, J. S. *Eur. J. Orghem.* **2000**, 2513–2528.
104. Brückner, R.; Priepke, H. *Angew. Chem.* **1988**, *100*, 285–286.
105. For a review, see: Nakai, T.; Tomooka, K. *Pure Appl. Chem.* **1997**, *69*, 595–600.
106. Bull, S. D.; Davies, S. G.; Hernández Dominguez, S.; Jones, S.; Price, A. J.; Sellers, T. G. R.; Smith, A. D. *J. Chem. Soc., Perkin Trans. 1* **2002**, 2141–2150.
107. Cox, L. R.; Ley, S. V. *Chem. Soc. Rev.* **1998**, *27*, 301–314 and references therein.
108. For a recent review of the chemistry of acyclic (diene)iron complexes, see: Donaldson, W. A.; Chaudhury, S. *Eur. J. Org. Chem.* **2009**, 3831–3843.
109. Williams, I.; Reeves, K.; Kariuki, B. M.; Cox, L. R. *Org. Biomol. Chem.* **2007**, *5*, 3325–3329.
110. Paley, R. S.; Berry, K. E.; Liu, J. M.; Sanan, T. T. *J. Org. Chem.* **2009**, *74*, 1611–1620.
111. Platżuk, D.; Zakrewski, J.; Rybarczyk-Pirek, A. *J. Organomet. Chem.* **2006**, *691*, 3098–3102.
112. Mucha, B.; Kłys, A.; Rybarczyk-Pirek, A.; Zakrewski, J. *Tetrahedron: Asymmetry* **2007**, *18*, 1766–1768.
113. (a) Lin, Y.-L.; Cheng, M.-H.; Chen, W.-C.; Peng, S.-M.; Wang, S.-L.; Kuo, H.; Liu, R.-S. *J. Org. Chem.* **2001**, *66*, 1781–1786; (b) Cheng, M.-H.; Ho, Y.-H.; Lee, G.-H.; Peng, S.-M.; Chu, S.-Y.; Liu, R.-S. *Organometallics* **1994**, *13*, 4082–4091.

Biographical sketch

Alex O'Brien received his M.Sc. in Chemistry from the University of Bristol in 2006, during which he spent a year at Bayer CropScience, Frankfurt am Main working in herbicide discovery and also carried out research at Bristol in the group of Dr Paul Wyatt. He then moved to Imperial College London for a DTA/Pfizer CASE funded Ph.D. under the supervision of Professor Donald Craig, studying the nature of acyclic stereocontrol in the Claisen rearrangement. Upon completion of his Ph.D. in 2010, he moved to a postdoctoral position with Professor Peter H. Seeberger at the Max Planck Institute for Colloids and Interfaces in Berlin. His current research focuses on the generation of high-energy reactive intermediates in microreactor systems.